PERGAMON

International Journal of Solids and Structures 36 (1999) 813–846

INTERNATIONAL JOURNAL OF SOLIDS and STRUCTURES

Delaminations induced by constrained transverse cracking in symmetric composite laminates

Junqian Zhang[a,]*, Jinghong Fan[a], K. P. Herrmann

[a] *Department of Engineering Mechanics, Chongqing University, 400044 Chongqing, P.R. China*

[b] *Laboratorium für Technische Mechanik, Universität Paderborn, 33098 Paderborn, Germany*

Received 29 January 1997; in revised form 9 October 1997

Abstract

Transverse ply cracking and its induced delaminations at the $\phi/90^\circ$ interfaces in $[\ldots/\varphi_i/\phi_m/90_n]_s$ laminates are theoretically investigated. Three cracked and delaminated model laminates, one five-layer model (FLM) laminate $[S^L/\phi_m/90_{2n}/\phi_m/S^R]_T$ and two three-layer model (TLM) laminates I and II, $[\phi_m/90_{2n}/\phi_m]_T$ and $[S'^L/90_{2n}/S'^R]_T$, are designed to examine constraining mechanisms of the constraining plies of the center 90°-ply group on transverse crack induced delaminations, where S^L, S^R, S'^L and S'^R are sublaminates $[\ldots/\varphi_i]_T$, $[\varphi_i/\ldots]_T$, $[\ldots/\varphi_i/\phi_m]_T$ and $[\phi_m/\varphi_i/\ldots]_T$, respectively. A sublaminate-wise first-order shear laminate theory is used to analyze stress and strain fields in the three cracked and delaminated laminates loaded in tension. The extension stiffness reduction of the constrained 90°-plies and the strain energy release rate for a local delamination normalized by the square of the laminate strain are calculated as a function of delamination length and transverse crack spacing. The constraining effects of the immediate neighboring plies and the remote plies are identified by conducting comparisons between the three model laminates. It is seen for the examined laminates that the nearest neighboring ply group of the 90°-plies primarily affects the stiffness reduction and also the normalized strain energy release rate, whereas the influences of the remote constraining layers are negligible. © 1998 Elsevier Science Ltd. All rights reserved.

1. Introduction

The fracture process of composite laminates under monotonic tension and tension fatigue loading involves sequential accumulation of damage in the form of matrix cracking, edge delamination and local delamination prior to catastrophic failure (see e.g. Jamison et al., 1984; Crossman and Wang, 1982; O'Brien, 1982, 1985). Local delamination initiates at matrix ply cracks due to a high interlaminar stress concentration at the crack tips whereas edge delamination originates from

* Corresponding author. Current address: Laboratorium für Technisch Mechanik, Universität Paderborn, 33098 Paderborn, Germany.

PII: S0020–7683(97)00035–9

the load-free edge of a composite plate. These through-thickness failure modes can be detrimental to the strength and stiffness of the composite laminates. It is therefore important to be in a position to predict their onset strain and growth.

Over the years many theories have been developed which attempt to model, with varying degree of sophistication, the laminate reduced properties and the strain energy release rates due to matrix cracking and its induced delamination (so-called local delamination). The strain energy release rate G associated with a local delamination can be compared with an appropriate value of the interlaminar fracture toughness, obtained experimentally (Martin and Murri, 1990), to estimate the initiation and propagation of such a delamination. The models could be categorized in terms of their adopted stress analysis methods used to calculate the stress distributions in the cracked laminates.

Based on shear-lag type arguments transverse ply cracking in cross-ply type laminates have been intensively modeled with varying emphases on the prediction of crack spacing saturation (Parvizi and Bailey, 1978), the statistical characteristic of crack formation (Fukanaga et al., 1984; Laws and Dvorak, 1988), determination of the shear-lag parameters and the in-plane stiffness reduction (Nuismer and Tan, 1988; Han and Hahn, 1989; Zhang et al., 1992a) as well as the influence of the stacking sequence (Zhang et al., 1992b; Xu, 1995). Dharani and Tang (1990) described a consistent shear-lag analysis to determine the interlaminar shear and normal stresses at the tips of matrix cracks inducing delaminations. Delamination occurs when the maximum interlaminar shear stress reaches a critical value. A numerical eigenvalue technique is required to solve the resulting governing equations. Zhang et al. (1994) have derived the closed-form expressions for the strain energy release rate and the stiffness reduction due to a local delamination where hygrothermal effects have also been taken into account. Comprehensive comparisons between this model, Nairn and Hu (1992) variational model and 2-D finite element method results have been carried out, suggesting that Zhang et al.'s more simple shear-lag model is accurate in comparison with Nairn–Hu's model. The problem with the shear-lag analyses is that the constraining layer (sublaminate) is assumed as a homogeneous medium without taking into account the stacking sequence effects (e.g. no difference between constraining layers $[0/45/-45]_T$ and $[45/-45/0]_T$).

The variational model based on the principle of minimum complementary energy was proposed by Hashin (1987) with application to the stiffness reduction and stress analysis of the cross-ply laminates with transverse ply cracking. Thereby the assumption of constant in-plane stresses across the thickness has been made. Nairn and Hu (1992) used the variational technique to predict multiple transverse ply cracking and the growth of a delamination induced by matrix cracking. Analyses of more general in-plane stresses and a non-linear stress distribution across the thickness were conducted by Varna and Berglund (1991). However, using a variational approach to calculate the stress field in a cracked laminate is more cumbersome than applying methods based on shear-lag type arguments. Again, by using the assumption of a homogeneous constraining layer makes it impossible to account for the influence of the stacking sequence of constraining sublaminates.

The third category of a stress analysis method is based on the laminate plate theories. O'Brien (1985) using the classical laminate plate theory and by assuming that the laminated portion and the delaminated interval carry loads in series, derived a closed-form equation for G, which for certain lay-ups can successfully predict the delamination onset strain. The model has been further extended to include the effect of residual thermal and moisture stresses on G (O'Brien, 1991). However, the author neglected the effect of matrix cracks which exist before a local delamination occurs. Armanios et al. (1991) developed a sublaminate approach for the analysis of a local delamination including the effect of residual hygrothermal stresses under plane strain conditions by utilizing the first-order shear deformation laminate plate theory. A cracked and delaminated cross-ply type laminate is divided into four sublaminates by the delamination interfacial surface and the cross-section to which the delamination tip reaches. The model was used to predict the onset of local delaminations in T300/934 graphite/epoxy $[\pm 25/90_n]_s$ laminates by utilizing Griffith's energy release rate criterion. Praveen and Reddy (1994) analyzed the stiffness reduction and interlaminar stresses of [0/90/0] type laminates with transverse ply cracks by using Reddy's layer-wise laminate theory and a complementary principle similar to that of Hashin (1987).

A three-dimensional (3-D) finite element analysis was performed by Salpekar and O'Brien (1991) to evaluate the energy release rate for local delaminations in glass fiber-reinforced plastic laminates containing 90° matrix cracks of large spacing and loaded in tension. It was observed that the value of the total G calculated near the free edge increased with increasing delamination length and approached O'Brien's (1985) closed-form solution for delamination lengths of about four ply thicknesses from the matrix crack. It was concluded that a convergence study, using several mesh refinements, is needed to make quantitative comparisons of the analytical solution with the 3-D finite element model. The influence of transverse ply crack spacing on the strain energy release rate associated with a local delamination was investigated numerically by performing a 2-D finite element analysis (Zhang et al., 1994). The G-value for a local delamination decreases notably with an increasing matrix cracking.

A few of the existing works only pay attention to a quantitative examination of constraining effects on the transverse ply cracking and its induced delamination. In this article the constraining influences of the nearest-neighboring ply group of the core 90°-plies and the rest constraining plies on the stiffness reduction of the constrained 90°-plies and on the strain energy release rate due to a local delamination are theoretically investigated. Firstly, three equivalent constraint model laminates, one five-layer model laminate and two three-layer model laminates, are proposed. The cracked and delaminated model laminates are then subdivided by the cross-section separating the laminated and delaminated intervals. Analyses of stress and strain fields are carried out by applying the first-order shear deformation laminate theory to each sublaminate. The in situ damage effective function (IDEF) Λ_{22}, introduced in our previous work (Zhang et al., 1992a, 1994) for characterizing the extension stiffness reduction of the constrained 90°-plies, is explicitly expressed in terms of delamination length and transverse crack spacing by using the obtained stress field. The strain energy release rate for a local delamination is derived as a function of delamination length and transverse crack spacing. The three model laminates are used to predict the stiffness reduction of the constrained 90°-plies and the normalized strain energy release rate due to a local delamination against the delamination length for a given transverse crack density for various stacking sequence laminates. A comparison between the three model laminates has been conducted.

2. Equivalent constraint model (ECM)

If a $[\ldots/\varphi_i/\phi_m/90_n]_s$ symmetric laminate is under static or fatigue tensile loading matrix cracking in the transverse plies (90°) is the first damage mode observed and multiplied by an increasing applied load. Subsequently, a local delamination could initiate from the transverse ply crack tips due to high local stresses at the crack tips. The through-width uniform local delaminations growing from 90°-ply matrix crack tips are assumed according to Fig. 1. The three-layer Equivalent Constraint Model (ECM) laminate for the 90°-ply cracking and its induced delaminations, proposed by Fan and Zhang (1993), Zhang et al. (1992a, 1994), consists of two stiffness-equivalent outer constraining sublaminates of $[\ldots/\varphi_i/\phi_m]_T$ and $[\phi_m/\varphi_i/\ldots]_T$ and the core ply group of $[90_{2n}]$, Fig. 1(c). The three-layer ECM model laminate II (Fig. 1(c)) is accurate enough to estimate the global properties of the laminates, e.g. a stiffness reduction, which are not very sensitive to the details of the micro configurations. However, delamination and cracking failure might depend strongly upon the local microstructure of a laminate. The nearest neighboring ply group (ϕ) of the 90°-plies could primarily affect the initiation and growth of transverse cracking as well as delamination at the $\phi/90°$ interface whereas the rest plies have a relatively smaller contribution to the constraining effect on these damage modes. In order to account for these hierarchical constraining mechanisms, a five-layer ECM model laminate $[S^L/\phi_m/90_{2n}/\phi_m/S^R]_T$ (Fig. 1(a)) and another three-layer model laminate $[\phi_m/90_{2n}/\phi_m]_T$ (designated by TLM I, Fig. 1(b)), where S^L and S^R are sublaminates $[\ldots/\varphi_i]_T$ and $[\varphi_i/\ldots]_T$, respectively, are introduced in addition to the three-layer model laminate proposed previously and designated by TLM II in Fig. 1(c)). Both the nearest neighboring ϕ-plies of the center 90°-plies are called two primary constraining layers and the two outer sublaminates S^L and S^R are secondary constraining layers. A comparison between the TLM I and the five-layer model (FLM) laminates can be used to investigate the effects of secondary constraining layers whereas TLM I laminates with a changing constraining ply orientation are applied for the identification of the influences of primary constraining plies. The effects of a local lay-up configuration on the stiffness reduction and the strain energy release rates due to a local delamination as well as a matrix cracking could be examined by conducting a comparison between the FLM and TLM II laminates.

3. Stress analysis of a five-layer model (FLM) laminate

Let the five-layer model laminate $[S^L/\phi_m/90_{2n}/\phi_m/\mathrm{S}^R]_T$ to be subjected to a tension load, Fig. 2(a). The matrix cracks are assumed to exist in the 90°-ply group with a uniform crack spacing of $2s$; local delaminations initiate and grow from both tips of each matrix and span the width of the specimen. Further for symmetry reasons only one quarter of the repeating interval of the laminate is modeled. The modeled portion length s is divided into six sublaminates as shown in Fig. 2(a) and the delamination length at the interfaces of $\phi/90°$ is denoted by l. The laminate beam model which results in a one-dimensional procedure is used here by assuming plane strain in the width direction, which to some extent represents the situation of the deformation behavior of the composite laminate interior. The sublaminates are referred to three local co-ordinate systems, respectively, with a common y-axis and their origins at the centers of the left cross-sections of the sublaminates 1, 2 and 3, Fig. 2. The displacements in y- and z-directions within each sublaminate are assumed to be of the form (Armanios et al., 1991)

$$v(y,z) = V(y)+z\beta(y) \tag{1a}$$

$$w = W(y) \tag{1b}$$

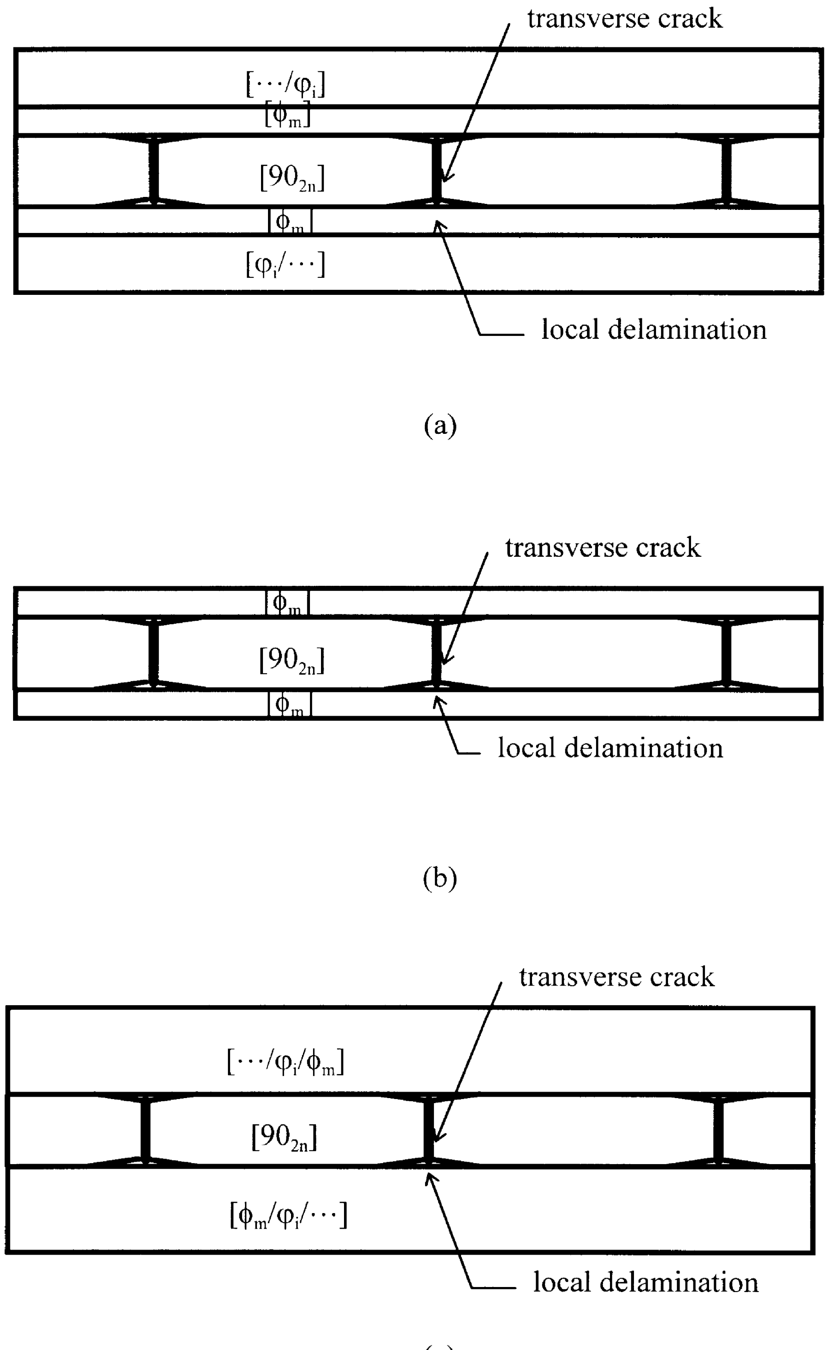

Fig. 1. Equivalent constraint model (ECM) laminates for the cracked and delaminated $[\ldots/\varphi_i/\phi_m/90_n]_s$ laminates: (a) a five-layer model (FLM) laminate; (b) a three-layer model laminate I (TLM I); (c) a three-layer model laminate II (TLM II).

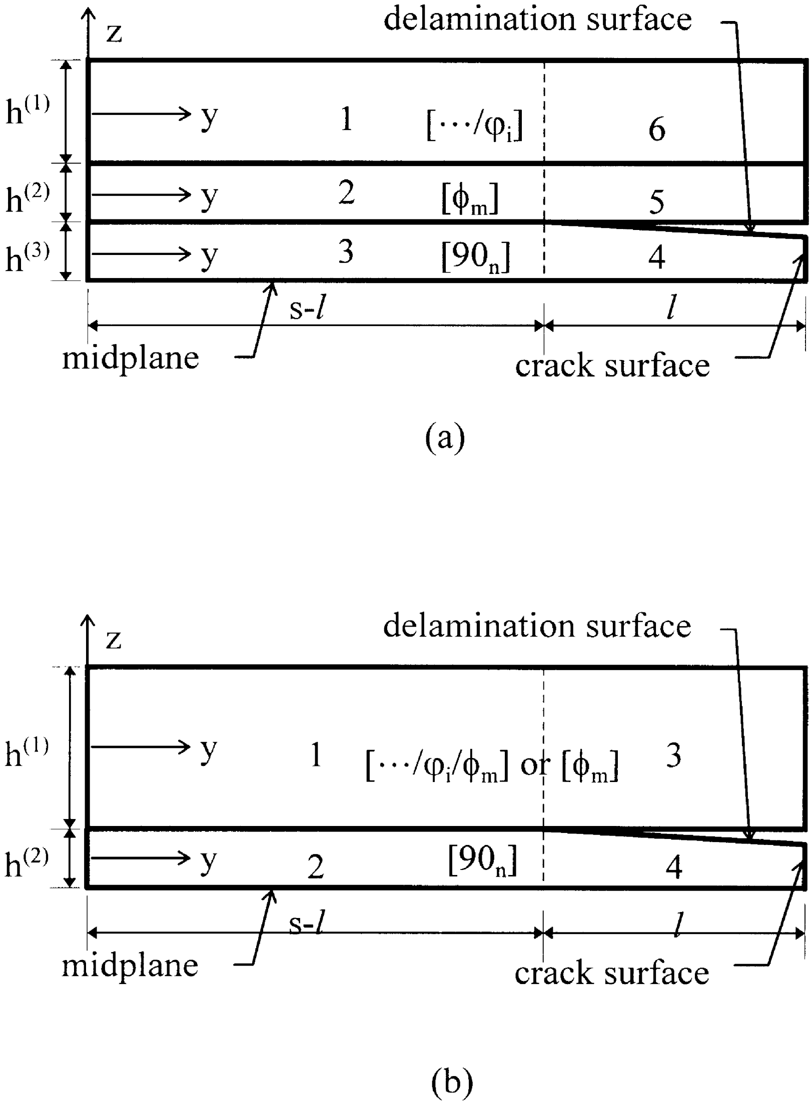

Fig. 2. Subdivision of a quarter the periodic interval of a $[\ldots/\varphi_i/\phi_m/90_n]_s$ laminate: (a) a five-layer model (FLM) laminate; (b) a three-layer model (TLM) laminate.

The shear deformation is recognized through the rotation $\beta(y)$. The equilibrium equations for each sublaminate take the form

$$N_{,y}+T_{\mathrm{t}}-T_{\mathrm{b}}=0 \tag{2a}$$

$$M_{,y}-Q+\frac{h}{2}(T_{\mathrm{t}}+T_{\mathrm{b}})=0 \tag{2b}$$

$$Q_{,y}+P_{\mathrm{t}}-P_{\mathrm{b}}=0 \tag{2c}$$

where N, Q and M are axial force, shear force and bending moment resultants at a cross-section; P and T denote the interlaminar peel and shear stresses; the subscripts "t" and "b" indicate the top and bottom surfaces; h is the thickness of a sublaminate. Using the strain-displacement relations, eqns (1a,b) and the in-plane stress–stain relationships of a lamina, the constitutive relationships of a sublaminate in terms of the force and moment resultants read as follows

$$N = A_{22}V_{,y} + B_{22}\beta_{,y} \tag{3a}$$

$$M = B_{22}V_{,y} + D_{22}\beta_{,y} \tag{3b}$$

$$Q = A_{44}(\beta + W_{,y}) \tag{3c}$$

where A_{22}, B_{22}, D_{22} and A_{44} are the extension, coupling, bending and out-of-plane shear stiffnesses, respectively, from the classical laminate theory. For the one-dimensional model the other stiffness components of the anisotropic sublaminate do not appear in the constitutive equations due to the assumption of plane strain with respect to the width of the specimen. Substitution of eqns (3a–c) into eqns (2a–c) gives

$$A_{22}V_{,yy} + B_{22}\beta_{,yy} + T_{\mathrm{t}} - T_{\mathrm{b}} = 0 \tag{4a}$$

$$\left(D_{22} - \frac{B_{22}^2}{A_{22}}\right)\beta_{,yy} - A_{44}(\beta + W_{,y}) + \left(\frac{h}{2} - \frac{B_{22}}{A_{22}}\right)T_{\mathrm{t}} + \left(\frac{h}{2} + \frac{B_{22}}{A_{22}}\right)T_{\mathrm{b}} = 0 \tag{4b}$$

$$A_{44}(\beta_{,y} + W_{,yy}) + P_{\mathrm{t}} - P_{\mathrm{b}} = 0 \tag{4c}$$

The quantities with a bracketed superscript "(i)" ($i = 1, 2, \ldots, 6$) to be used afterward belong to the respective sublaminate.

3.1. *Laminated portion* ($0 \leqslant y \leqslant s - l$)

The continuity conditions of the displacements at the interlaminar surfaces between the sublaminates 1 and 2, and the sublaminates 2 and 3 read in the laminated interval

$$V^{(1)}(y) - \frac{h^{(1)}}{2}\beta^{(1)}(y) = V^{(2)}(y) + \frac{h^{(2)}}{2}\beta^{(2)}(y) \tag{5a}$$

$$V^{(2)}(y) - \frac{h^{(2)}}{2}\beta^{(2)}(y) = V^{(3)}(y) + \frac{h^{(3)}}{2}\beta^{(3)}(y) \tag{5b}$$

$$W^{(1)}(y) = W^{(2)}(y) = W^{(3)}(y) = 0 \tag{5c}$$

Applying eqns (4a–c) to every sublaminate and by using eqn (5c), one can obtain

$$A_{22}^{(1)}V_{,yy}^{(1)} + B_{22}^{(1)}\beta_{,yy}^{(1)} - T_{\mathrm{b}}^{(1)} = 0 \tag{6a}$$

$$A_{22}^{(2)}V_{,yy}^{(2)} + T_{\mathrm{t}}^{(2)} - T_{\mathrm{b}}^{(2)} = 0 \tag{6b}$$

$$A_{22}^{(3)}V_{,yy}^{(3)} + T_{\mathrm{t}}^{(3)} = 0 \tag{6c}$$

$$\left(D_{22}^{(1)}-\frac{B_{22}^{(1)^2}}{A_{22}^{(1)}}\right)\beta_{,yy}^{(1)}-A_{44}^{(1)}\beta^{(1)}+\left(\frac{h^{(1)}}{2}+\frac{B_{22}^{(1)}}{A_{22}^{(1)}}\right)T_{\mathrm{b}}^{(1)}=0 \tag{6d}$$

$$D_{22}^{(2)}\beta_{,yy}^{(2)}-A_{44}^{(2)}\beta^{(2)}+\frac{h^{(2)}}{2}(T_{\mathrm{t}}^{(2)}+T_{\mathrm{b}}^{(2)})=0 \tag{6e}$$

$$D_{22}^{(3)}\beta_{,yy}^{(3)}-A_{44}^{(3)}\beta^{(3)}+\frac{h^{(3)}}{2}T_{\mathrm{t}}^{(3)}=0 \tag{6f}$$

$$A_{44}^{(1)}\beta_{,y}^{(1)}-P_{\mathrm{b}}^{(1)}=0 \tag{6g}$$

$$A_{44}^{(2)}\beta_{,y}^{(2)}+P_{\mathrm{t}}^{(2)}-P_{\mathrm{b}}^{(2)}=0 \tag{6h}$$

$$A_{44}^{(3)}\beta_{,y}^{(3)}+P_{\mathrm{t}}^{(3)}-P_{\mathrm{b}}^{(3)}=0 \tag{6i}$$

where the load-free assumption at the top surface and the condition of zero interfacial shear stress at the midplane have been used. By using the continuity conditions for the interfacial stresses one can solve eqns (5a,b) and (6a–c) in order to express $V_{,yy}^{(i)}$ and $T_{\mathrm{b}}^{(i)}$ in terms of the sublaminate rotation $\beta_{,yy}^{(i)}$ (see Appendix 1). Then, the substitution of these quantities into eqns (6d–f) results in (see Appendix 1)

$$\begin{bmatrix} a_{11} & a_{12} & a_{13} \\ a_{21} & a_{22} & a_{23} \\ a_{31} & a_{32} & a_{33} \end{bmatrix}\begin{Bmatrix}\beta_{,yy}^{(1)}\\ \beta_{,yy}^{(2)}\\ \beta_{,yy}^{(3)}\end{Bmatrix}-\begin{bmatrix} A_{44}^{(1)} & 0 & 0 \\ 0 & A_{44}^{(2)} & 0 \\ 0 & 0 & A_{44}^{(3)} \end{bmatrix}\begin{Bmatrix}\beta^{(1)}\\ \beta^{(2)}\\ \beta^{(3)}\end{Bmatrix}=0 \tag{7}$$

where a_{ij} are functions of the elastic constants of a lamina and of the lay-up parameters (see Appendix 3). Further, the characteristic equation corresponding to eqns (7) reads as follows:

$$\begin{aligned}&(a_{11}a_{22}a_{33}+2a_{12}a_{13}a_{23}-a_{33}a_{12}^2-a_{11}a_{23}^2-a_{22}a_{13}^2)\lambda^{*3}\\ &\quad-(a_{11}a_{22}A_{44}^{(3)}+a_{33}a_{22}A_{44}^{(1)}+a_{33}a_{11}A_{44}^{(2)}-a_{12}^2A_{44}^{(3)}-a_{23}^2A_{44}^{(1)}-a_{13}^2A_{44}^{(2)})\lambda^{*2}\\ &\quad+(a_{11}A_{44}^{(2)}A_{44}^{(3)}+a_{22}A_{44}^{(1)}A_{44}^{(3)}+a_{33}A_{44}^{(2)}A_{44}^{(1)})\lambda^{*}-A_{44}^{(1)}A_{44}^{(2)}A_{44}^{(3)}=0\end{aligned} \tag{8}$$

Its three roots λ_j^* $(j=1,2,3)$ are positive real numbers for all laminates examined here. The eigenvector $\{p_j\}=(p_j^{(1)}\quad p_j^{(2)}\quad 1)^T$ corresponding to the eigenvalue λ_j^* is given as

$$\begin{Bmatrix}p_j^{(1)}\\ p_j^{(2)}\end{Bmatrix}=\frac{\lambda_j^*}{(a_{11}\lambda_j^*-A_{44}^{(1)})(a_{22}\lambda_j^*-A_{44}^{(2)})-a_{12}^2\lambda^{*2}_j}\begin{Bmatrix}a_{13}A_{44}^{(2)}-(a_{22}a_{13}-a_{12}a_{23})\lambda_j^*\\ a_{23}A_{44}^{(1)}-(a_{11}a_{23}-a_{12}a_{13})\lambda_j^*\end{Bmatrix}\quad \text{for } j=1,2,3 \tag{9}$$

Using the condition of $\beta(y)=-\beta(-y)$ for the sublaminates 1, 2 and 3 the solutions $\beta^{(i)}$ in the governing eqns (7) read

$$\beta^{(i)}=\sum_{j=1}^{3}\alpha_j p_j^{(i)}\sinh(\lambda_j y)\quad \text{for } i=1,2,3 \tag{10}$$

where $\lambda_j = \sqrt{\lambda_j^*}$, and the parameters α_j are undetermined constants. Substituting equation (10) into eqns (A1.5a–c) gives

$$V^{(i)} = \sum_{j=1}^{3} \alpha_j \gamma_j^{(i)} \sinh(\lambda_j y) + \alpha_{3+i} y \quad \text{for } i = 1, 2, 3 \tag{11}$$

where $\gamma_j^{(i)}$ are constants (see Appendix 3) and α_4, α_5 and α_6 are undetermined constants. Substituting eqns (10) and (11) into eqns (3a–c) and (A1.4a,b) gives

$$N^{(i)} = \sum_{j=1}^{3} \alpha_j \eta_j^{(i)} \cosh(\lambda_j y) + A_{22}^{(i)} \alpha_{3+i} \quad \text{for } i = 1, 2, 3 \tag{12}$$

$$M^{(i)} = \sum_{j=1}^{3} \alpha_j \xi_j^{(i)} \cosh(\lambda_j y) + B_{22}^{(i)} \alpha_{3+i} \quad \text{for } i = 1, 2, 3 \tag{13}$$

$$T_{\rm b}^{(1)} = T_{\rm t}^{(2)} = \sum_{j=1}^{3} \alpha_j \lambda_j^2 (A_{22}^{(1)} \gamma_j^{(1)} + B_{22}^{(1)} p_j^{(1)}) \sinh(\lambda_j y) \tag{14}$$

$$T_b^{(2)} = T_{\rm t}^{(3)} = -A_{22}^{(3)} \sum_{j=1}^{3} \alpha_j \gamma_j^{(3)} \lambda_j^2 \sinh(\lambda_j y) \tag{15}$$

where the constants $\eta_j^{(i)}$ and $\xi_j^{(i)}$ are given in Appendix 3.

3.2. *Sublaminates "5" and "6"* ($s - l \leqslant y \leqslant s$)

The displacement continuity conditions between sublaminate "5" and "6" are

$$V^{(6)}(y) - \frac{h^{(1)}}{2} \beta^{(6)}(y) = V^{(5)}(y) + \frac{h^{(2)}}{2} \beta^{(5)}(y) \tag{16a}$$

$$W^{(5)}(y) = W^{(6)}(y) \tag{16b}$$

The shear and normal stresses at the surfaces and the interface satisfy the following conditions

$$T_{\rm t}^{(6)} = 0, \quad T_{\rm b}^{(6)} = T_{\rm t}^{(5)}, \quad T_{\rm b}^{(5)} = 0 \tag{17a,b,c}$$

$$P_{\rm t}^{(6)} = 0, \quad P_{\rm t}^{(5)} = P_{\rm b}^{(6)}, \quad P_{\rm b}^{(5)} = 0 \tag{17d,e,f}$$

Applying eqns (4a,b,c) to every sublaminate and by noting eqns (17a)–(17f), one can obtain

$$A_{22}^{(1)} V_{,yy}^{(6)} + B_{22}^{(1)} \beta_{,yy}^{(6)} - T_{\rm b}^{(6)} = 0 \tag{18a}$$

$$A_{22}^{(2)} V_{,yy}^{(5)} + T_{\rm t}^{(5)} = 0 \tag{18b}$$

$$\left(D_{22}^{(1)} - \frac{B_{22}^{(1)^2}}{A_{22}^{(1)}}\right) \beta_{,yy}^{(6)} - A_{44}^{(1)} (\beta^{(6)} + W_{,y}^{(6)}) + \left(\frac{h^{(1)}}{2} + \frac{B_{22}^{(1)}}{A_{22}^{(1)}}\right) T_{\rm b}^{(6)} = 0 \tag{18c}$$

$$D_{22}^{(2)} \beta_{,yy}^{(5)} - A_{44}^{(2)} (\beta^{(5)} + W_{,y}^{(5)}) + \frac{h^{(2)}}{2} T_{\rm t}^{(5)} = 0 \tag{18d}$$

$$A_{44}^{(1)}(\beta_{,y}^{(6)}+W_{,yy}^{(6)})+A_{44}^{(2)}(\beta_{,y}^{(5)}+W_{,yy}^{(5)}) = 0 \tag{18e}$$

By integrating the eqn (18e) and by using the continuity relation (16b), the boundary condition of $(Q^{(5)}+Q^{(6)})_{y=s} = 0$ and the constitutive relation, eqn (3c), result in

$$W_{,y}^{(5)} = W_{,y}^{(6)} = -\frac{1}{A_{44}^{(1)}+A_{44}^{(2)}}(A_{44}^{(1)}\beta^{(6)}+A_{44}^{(2)}\beta^{(5)}) \tag{19}$$

Further, the combination of eqns (16a), (17b) and (18a,b) results in

$$T_{\rm b}^{(6)} = T_{\rm t}^{(5)} = \frac{A_{22}^{(2)}}{2(A_{22}^{(1)}+A_{22}^{(2)})}[h^{(2)}A_{22}^{(1)}\beta_{,yy}^{(5)}+(h^{(1)}A_{22}^{(1)}+2B_{22}^{(1)})\beta_{,yy}^{(6)}] \tag{20a}$$

$$V_{,yy}^{(6)} = \frac{1}{2(A_{22}^{(1)}+A_{22}^{(2)})}[h^{(2)}A_{22}^{(2)}\beta_{,yy}^{(5)}+(h^{(1)}A_{22}^{(2)}-2B_{22}^{(1)})\beta_{,yy}^{(6)}] \tag{20b}$$

$$V_{,yy}^{(5)} = -\frac{1}{2(A_{22}^{(1)}+A_{22}^{(2)})}[h^{(2)}A_{22}^{(1)}\beta_{,yy}^{(5)}+(h^{(1)}A_{22}^{(1)}+2B_{22}^{(1)})\beta_{,yy}^{(6)}] \tag{20c}$$

By substituting eqns (19) and (20a) into eqns (18c,d) gives

$$\begin{bmatrix} b_{11} & b_{12} \\ b_{21} & b_{22} \end{bmatrix}\begin{Bmatrix} \beta_{,yy}^{(5)} \\ \beta_{,yy}^{(6)} \end{Bmatrix}+\frac{A_{44}^{(1)}A_{44}^{(2)}}{A_{44}^{(1)}+A_{44}^{(2)}}\begin{bmatrix} -1 & 1 \\ 1 & -1 \end{bmatrix}\begin{Bmatrix} \beta^{(5)} \\ \beta^{(6)} \end{Bmatrix} = 0 \tag{21}$$

where b_{ij} are functions of the elastic lamina properties and the lay-up parameters (see Appendix 3). The general solutions of eqn (21) are written as

$$\begin{Bmatrix} \beta^{(5)} \\ \beta^{(6)} \end{Bmatrix} = \theta_1\, e^{\omega y}\begin{Bmatrix} q \\ 1 \end{Bmatrix}+\theta_2\, e^{-\omega y}\begin{Bmatrix} q \\ 1 \end{Bmatrix}+\theta_3 y\begin{Bmatrix} 1 \\ 1 \end{Bmatrix}+\theta_4\begin{Bmatrix} 1 \\ 1 \end{Bmatrix} \tag{22}$$

where ω is the non-zero eigenvalue of eqn (21) and is given by

$$\omega = \sqrt{\frac{A_{44}^{(1)}A_{44}^{(2)}(b_{11}+b_{22}+2b_{12})}{(A_{44}^{(1)}+A_{44}^{(2)})(b_{11}b_{22}-b_{12}^2)}} \tag{23a}$$

and

$$q = -\frac{b_{22}+b_{12}}{b_{11}+b_{12}} \tag{23b}$$

By integrating eqns (19) and (20b,c) and by substituting eqn (22) into them result in

$$V^{(5)} = -k_1(\theta_1\, e^{\omega y}+\theta_2\, e^{-\omega y})+\theta_5 y+\theta_7 \tag{24a}$$

$$V^{(6)} = k_3(\theta_1\, e^{\omega y}+\theta_2\, e^{-\omega y})+\theta_6 y+\theta_8 \tag{24b}$$

$$W^{(5)} = W^{(6)} = -\frac{A_{44}^{(1)}+qA_{44}^{(2)}}{\omega(A_{44}^{(1)}+A_{44}^{(2)})}(\theta_1\, e^{\omega y}-\theta_2\, e^{-\omega y})-\frac{1}{2}\theta_3 y^2-\theta_4 y+\theta_9 \tag{24c}$$

Introducing eqns (22) and (24a,b) into eqns (3a–c) gives

$$N^{(5)} = -k_1 A_{22}^{(2)} \omega(\theta_1 e^{\omega y} - \theta_2 e^{-\omega y}) + A_{22}^{(2)} \theta_5 \tag{25a}$$

$$N^{(6)} = k_1 A_{22}^{(2)} \omega(\theta_1 e^{\omega y} - \theta_2 e^{-\omega y}) + A_{22}^{(1)} \theta_6 + B_{22}^{(1)} \theta_3 \tag{25b}$$

$$M^{(5)} = k_2(\theta_1 e^{\omega y} - \theta_2 e^{-\omega y}) + D_{22}^{(2)} \theta_3 \tag{25c}$$

$$M^{(6)} = \omega(D_{22}^{(1)} + B_{22}^{(1)} k_3)(\theta_1 e^{\omega y} - \theta_2 e^{-\omega y}) + D_{22}^{(1)} \theta_3 + B_{22}^{(1)} \theta_6 \tag{25d}$$

where the k_i are given in Appendix 3.

3.3. *Sublaminate 4* ($s - l \leqslant y \leqslant s$)

The symmetry of the laminate implies

$$W^{(4)}(y) = 0, \quad T_{\mathrm{b}}^{(4)} = 0 \tag{26a,b}$$

The condition of the traction-freedom at the upper surface of the sublaminate 4 reads

$$T_{\mathrm{t}}^{(4)} = 0 \quad P_{\mathrm{t}}^{(4)} = 0 \tag{26c,d}$$

By applying eqns (4a,b,c) to the sublaminate 4 and by noting eqns (26a–d), one can obtain

$$A_{22}^{(3)} V_{,yy}^{(4)} = 0 \tag{27a}$$

$$D_{22}^{(3)} \beta_{,yy}^{(4)} - A_{44}^{(3)} \beta^{(4)} = 0 \tag{27b}$$

$$A_{44}^{(3)} \beta_{,y}^{(4)} - P_{\mathrm{b}}^{(4)} = 0 \tag{27c}$$

The general solutions of eqns (27a,b) are

$$\beta^{(4)} = \psi_1 e^{\omega_1 y} + \psi_2 e^{-\omega_1 y} \tag{28a}$$

$$V^{(4)} = \psi_3 y + \psi_4 \tag{28b}$$

where

$$\omega_1 = \sqrt{\frac{A_{44}^{(3)}}{D_{22}^{(3)}}} \tag{28c}$$

The substitution of eqns (28a,b) into the constitutive eqns (3a,b) results in

$$N^{(4)} = A_{22}^{(3)} \psi_3 \tag{29a}$$

$$M^{(4)} = D_{22}^{(3)} \omega_1 (\psi_1 e^{-\omega_1 y} - \psi_2 e^{-\omega_1 y}) \tag{29b}$$

3.4. *Determination of the constants* α_i, θ_j *and* ψ_k

In order to determine the nineteen constants of α_i ($i = 1, 2, \ldots, 6$), θ_j ($j = 1, 2, \ldots, 9$) and ψ_k ($k = 1, 2, 3, 4$) the same number of independent boundary and continuity conditions have to be prescribed. Assuming the laminate subjected to a tension force, N, the boundary conditions at the ends of the model laminate are enforced as

$$N^{(4)}(s) = 0 \quad \beta^{(5)}(s) = 0 \quad \beta^{(6)}(s) = 0 \tag{30a,b,c}$$

$$V^{(5)}(s) = V^{(6)}(s) \quad N^{(5)}(s)+N^{(6)}(s) = \tfrac{1}{2}N \tag{30d,e}$$

$$N^{(1)}(0)+N^{(2)}(0)+N^{(3)}(0) = \tfrac{1}{2}N \tag{30f}$$

The interfacial displacement continuity eqns (5a,b) have to be checked by substitution of the midplane displacement and rotation solutions [eqns (10) and (11)] for the determination of the unknown constants because what have been used in the derivation of the governing eqn (7) are the second derivatives of such interface displacement continuity equations instead of themselves.

The displacement continuity conditions between the ends of the sublaminates read

$$V^{(1)}(s-l) = V^{(6)}(s-l) \quad V^{(2)}(s-l) = V^{(5)}(s-l) \tag{31a,b}$$

$$V^{(3)}(s-l) = V^{(4)}(s-l) \quad \beta^{(1)}(s-l) = \beta^{(6)}(s-l) \tag{31c,d}$$

$$\beta^{(2)}(s-l) = \beta^{(5)}(s-l) \quad \beta^{(3)}(s-l) = \beta^{(4)}(s-l) \tag{31e,f}$$

$$W^{(5)}(s-l) = 0 \tag{31g}$$

In addition, the force and moment resultants, N and M (or the first-order derivatives of the midplane displacement and rotation, $V_{,y}$ and $\beta_{,y}$) are enforced to be continuous at the cross-section $y = s-l$

$$N^{(2)}(s-l) = N^{(5)}(s-l) \quad N^{(3)}(s-l) = N^{(4)}(s-l) \tag{31h,i}$$

$$M^{(2)}(s-l) = M^{(5)}(s-l) \quad M^{(3)}(s-l) = M^{(4)}(s-l) \tag{31j,k}$$

The continuity conditions of the force and moment resultants, N and M, between the sublaminates 1 and 6 are not needed to be specified since they can be derived by combining eqns (30a,e,f) and (31h–j) with eqns (3a,b), (5a) and (16a). The following equations for determining α_j ($j = 1, 2, \ldots, 6$) can be obtained from eqns (30a–f), (5a,b) and (31a–k) (see Appendix 2)

$$[F]\{\bar{\alpha}\} = \{R\} \tag{32a}$$

$$\alpha_4 = \alpha_5 = \alpha_6 = \frac{N}{A_{22}} \tag{32b}$$

where A_{22} is the extension stiffness of an undamaged laminate, and the elements of the third-order matrix $[F]_{3\times 3}$, vectors $\{\bar{\alpha}\}_3$ and $\{R\}_3$ are

$$\alpha_j = -\bar{\alpha}_j \frac{N}{A_{22}\cosh(\lambda_j(s-l))} \tag{33a}$$

$$F_{1j}(l, s-l) = 2\rho_j(1-q)\tanh(\omega l)+(p_j^{(1)}-p_j^{(2)})\tanh(\lambda_j(s-l)) \tag{33b}$$

$$F_{2j}(l, s-l) = (1-q)\delta_j l-(p_j^{(1)}q-p_j^{(2)})\tanh(\lambda_j(s-l)) \tag{33c}$$

$$F_{3j}(l, s-l) = \eta_j^{(3)} \tag{33d}$$

for $j = 1, 2, 3$.

$$R_1 = 2(1-q)\tanh(\omega l)k_7 \tag{34a}$$

$$R_2 = (1-q)k_6 l \tag{34b}$$

$$R_3 = A_{22}^{(3)} \tag{34c}$$

The other undetermined constants expressed in terms of α_j ($j = 1, 2, 3$) are given in Appendix 2.

4. Stress analysis of a three-layer model (TLM) laminate

A quarter of the cracked and delaminated TLM laminate is segregated into four sublaminates as it has been done by Armonios et al. (1991), Fig. 2(b). The procedure for analyzing the three-layer ECM model laminate is similar to that for the five-layer ECM model laminate. Therefore, only the final results are outlined here. The quantities calculated by the three-layer models are marked by a superscript "′". The eqns (1)–(4) are also valid for the three-layer sublaminate analysis.

4.1. *Laminated region* ($0 \leqslant y \leqslant s-l$)

Using displacement and stress continuity conditions at the interface between the sublaminates 1 and 2 in the three-layer model laminate, the application of eqns (4a–c) to the laminated interval results in the following governing equations

$$\begin{bmatrix} a'_{11} & a'_{12} \\ a'_{21} & a'_{22} \end{bmatrix} \begin{Bmatrix} \beta'^{(1)}_{,yy} \\ \beta'^{(2)}_{,yy} \end{Bmatrix} - \begin{bmatrix} A'^{(1)}_{44} & 0 \\ 0 & A'^{(2)}_{44} \end{bmatrix} \begin{Bmatrix} \beta'^{(1)} \\ \beta'^{(2)} \end{Bmatrix} = 0 \tag{35}$$

where the a'_{ij} listed in Appendix 4 are laminate constants. The eigenvalues of the corresponding characteristic equation are real for the examined laminates. The two positive roots are denoted by λ'_1 and λ'_2 given in Appendix 4. The solutions of the above equations are

$$\beta'^{(1)} = \alpha'_1 p'_1 \sinh(\lambda'_1 y) + \alpha'_2 p'_2 \sinh(\lambda'_2 y) \tag{36a}$$

$$\beta'^{(2)} = \alpha'_1 \sinh(\lambda'_1 y) + \alpha'_2 \sinh(\lambda'_2 y) \tag{36b}$$

where the p'_i are laminate constants listed in Appendix 4 and the α'_i are undetermined constants. The displacements of the midplane of the sublaminates are

$$V'^{(1)} = \alpha'_1 \gamma'^{(1)}_1 \sinh(\lambda'_1 y) + \alpha'_2 \gamma'^{(1)}_2 \sinh(\lambda'_2 y) + \alpha'_3 y \tag{37a}$$

$$V'^{(2)} = \alpha'_1 \gamma'^{(2)}_1 \sinh(\lambda'_1 y) + \alpha'_2 \gamma'^{(2)}_2 \sinh(\lambda'_2 y) + \alpha'_4 y \tag{37b}$$

The force and moment resultants read

$$N'^{(1)} = \alpha'_1 \eta'_2 \cosh(\lambda'_1 y) + \alpha'_2 \eta'_2 \cosh(\lambda'_2 y) + A'^{(1)}_{22} \alpha'_3 \tag{38a}$$

$$N'^{(2)} = -\alpha'_1 \eta'_1 \cosh(\lambda'_1 y) - \alpha'_2 \eta'_2 \cosh(\lambda'_2 y) + A'^{(2)}_{22} \alpha'_4 \tag{38b}$$

$$M'^{(1)} = \alpha'_1 \xi'^{(1)}_1 \cosh(\lambda'_1 y) + \alpha'_2 \xi'^{(1)}_2 \cosh(\lambda'_2 y) + B'^{(1)}_{22} \alpha'_3 \tag{38c}$$

$$M'^{(2)} = \alpha'_1 \xi'^{(2)}_1 \cosh(\lambda'_1 y) + \alpha'_2 \xi'^{(2)}_2 \cosh(\lambda'_2 y) \tag{38d}$$

where the laminate constants $\gamma'^{(i)}_j$, η'_j and $\xi'^{(i)}_j$ are given in Appendix 4.

4.2. *Sublaminate* 3 $(s-l \leqslant y \leqslant s)$

The governing equations can be obtained by applying eqns (4a–c) to the sublaminate 3 as follows

$$A'^{(1)}_{22} V'^{(3)}_{,yy} + B'^{(1)}_{22} \beta'^{(3)}_{,yy} = 0 \quad \beta'^{(3)}_{,yy} = 0 \tag{39a,b}$$

By solving eqns (39a,b) gives

$$\beta'^{(3)} = \theta'_1 y + \theta'_2 \quad V'^{(3)} = \theta'_3 y + \theta'_4 \tag{40a,b}$$

The substitution of eqns (40a,b) into eqns (3a,b) results in

$$N'^{(3)} = A'^{(1)}_{22} \theta'_3 + B'^{(1)}_{22} \theta'_1 \quad M'^{(3)} = B'^{(1)}_{22} \theta'_3 + D'^{(1)}_{22} \theta'_1 \tag{41a,b}$$

4.3. *Sublaminate* 4 $(s-l \leqslant y \leqslant s)$

The displacement and force solutions for the sublaminate 4 in the three-layer model laminate are exactly of the same shape as those for the sublaminate 4 in the five-layer model laminate. They are re-written as follows

$$\beta'^{(4)} = \psi'_1 e^{\omega'_1 y} + \psi'_2 e^{-\omega'_1 y} \quad V'^{(4)} = \psi'_3 y + \psi'_4 \tag{42a,b}$$

$$N'^{(4)} = A'^{(2)}_{22} \psi'_3 \quad M'^{(4)} = D'^{(2)}_{22} \omega'_1 (\psi'_1 e^{\omega'_1 y} - \psi'_2 e^{-\omega'_1 y}) \tag{42c,d}$$

where

$$\omega'_1 = \sqrt{\frac{A'^{(2)}_{44}}{D'^{(2)}_{22}}} \tag{42e}$$

4.4. *Determination of the constants* α'_i, θ'_j, *and* ψ'_k

The twelve end and interfacial continuity conditions are enforced as follows in order to determine the twelve undetermined constants

$$\beta'^{(3)}(s) = 0 \quad N'^{(3)}(s) = \tfrac{1}{2} N \tag{43a,b}$$

$$N'^{(1)}(0) + N'^{(2)}(0) = \tfrac{1}{2} N \quad N'^{(4)}(s) = 0 \tag{43c,d}$$

$$v^{(1)}\left(y, -\frac{h'^{(1)}}{2}\right) = v'^{(2)}\left(y, \frac{h'^{(2)}}{2}\right) \quad V'^{(1)}(s-l) = V'^{(3)}(s-l) \tag{43e,f}$$

$$V'^{(2)}(s-l) = V'^{(4)}(s-l) \quad \beta'^{(1)}(s-l) = \beta'^{(3)}(s-l) \tag{43g,h}$$

$$\beta'^{(2)}(s-l) = \beta'^{(4)}(s-l) \quad N'^{(2)}(s-l) = N'^{(4)}(s-l) \tag{43i,j}$$

$$M'^{(1)}(s-l) = M'^{(3)}(s-l) \quad M'^{(2)}(s-l) = M'^{(4)}(s-l) \tag{43k,l}$$

The determination of the constants α'_j $(j = 1, 2, 3, 4)$ can be reduced due to a substitution of the solutions for V', β', N' and M' into eqns (43a–l)

$$\begin{bmatrix} F'_{11} & F'_{12} \\ \eta_1 & \eta_2 \end{bmatrix} \begin{Bmatrix} \bar{\alpha}'_1 \\ \bar{\alpha}'_2 \end{Bmatrix} = -\begin{Bmatrix} B'^{(1)}_{22}\chi' l \\ A'^{(2)}_{22} \end{Bmatrix} \tag{44a}$$

$$\alpha'_3 = \alpha'_4 = \frac{N}{A'_{22}} \tag{44b}$$

where

$$F'_{1j} = \xi'^{(1)}_j l + \left(D'^{(1)}_{22} - \frac{B'^{(1)^2}_{22}}{A'^{(1)}_{22}} \right) p'_j \tanh(\lambda'_j(s-l)) \tag{45a}$$

$$\alpha'_j = -\bar{\alpha}'_j \frac{N}{A'_{22}\cosh(\lambda'_j(s-l))} \tag{45b}$$

for $j = 1, 2$. The other undetermined constants θ'_j and ψ'_k are expressed in terms of α'_i in Appendix 4.

5. Stiffness reduction

Since the rotation of the end-section of the constraining layers in both the five-layer model (FLM) and the three-layer model (TLM) laminates is zero, the overall laminate axial strain can be defined as follows

$$\varepsilon_y = \frac{V^{(6)}(s)}{s} = \frac{V^{(5)}(s)}{s} = \frac{\theta_5 s + \theta_7}{s} = \frac{\theta_6 s + \theta_8}{s} \quad \text{for FLM} \tag{46a}$$

$$\varepsilon_y = \frac{V'^{(3)}(s)}{s} = \frac{\theta'_3 s + \theta'_4}{s} \quad \text{for TLM} \tag{46b}$$

Consequently, the extension stiffness of a damaged laminate in y-direction is given by

$$A^{\mathrm{d}}_{22} = \frac{N}{\varepsilon_y} \tag{47}$$

Using eqn (A2.13c) the reduced extension stiffness can be expressed as a function of the delamination length and the transverse crack spacing

$$A^{\mathrm{d}}_{22} = \frac{A_{22}}{1 + \chi\left(\dfrac{l}{s} + \sum_{j=1}^{3} \bar{\alpha}_j \gamma_j^{(3)} \dfrac{\tanh(\lambda_j(s-l))}{s} \right)} \quad \text{for FLM} \tag{48a}$$

$$A'^{\mathrm{d}}_{22} = \frac{A'_{22}}{1+\chi'\left(\frac{l}{s}+\sum_{j=1}^{2}\bar{\alpha}'_j\gamma'^{(2)}_j\frac{\tanh(\lambda'_j(s-l))}{s}\right)} \quad \text{for TLM} \tag{48b}$$

In the context of the Equivalent Constraint Model (ECM), the stiffness reduction of the laminate due to transverse cracking and its induced delamination is assumed to be attributed to the loss of the load-carrying capacity of the 90°-plies. The reduced stiffness of the 90°-ply group normalized by the stiffness of an intact lamina, called in situ damage effective function (IDEF), Λ_{ij}, was introduced by Zhang et al. (1992a, 1994). It can be determined by assuming that the stiffness of an "equivalent" laminate where the degraded 90°-plies are perfectly bounded is equal to that of the real cracked and delaminated laminate, i.e.

$$\Lambda_{22} = \frac{A_{22}-A^{\mathrm{d}}_{22}}{2A^{(3)}_{22}} \quad \text{for FLM} \tag{49a}$$

$$\Lambda'_{22} = \frac{A'_{22}-A'^{\mathrm{d}}_{22}}{2A'^{(2)}_{22}} \quad \text{for TLM} \tag{49b}$$

Zero or unity values of the IDEF reflect constancy or total loss of the load-carrying capacity of the 90°-plies, respectively. Substitution of eqns (A3.1a), (A.4.1a) and (48a,b) results in the following expressions:

$$\Lambda_{22} = \frac{(1+\chi)\left[\frac{l}{s}+\sum_{j=1}^{3}\bar{\alpha}_j\gamma^{(3)}_j\frac{\tanh(\lambda_j(s-l))}{s}\right]}{1+\chi\left[\frac{l}{s}+\sum_{j=1}^{3}\bar{\alpha}_j\gamma^{(3)}_j\frac{\tanh(\lambda_j(s-l)}{s}\right]} \quad \text{for FLM} \tag{50a}$$

$$\Lambda'_{22} = \frac{(1+\chi')\left[\frac{l}{s}+\sum_{j=1}^{2}\bar{\alpha}'_j\gamma'^{(2)}_j\frac{\tanh(\lambda'_j(s-l))}{s}\right]}{1+\chi'\left[\frac{l}{s}+\sum_{j=1}^{2}\bar{\alpha}'_j\gamma'^{(2)}_j\frac{\tanh(\lambda'_j(s-l))}{s}\right]} \quad \text{for TLM} \tag{50b}$$

The quantities Λ_{22} and Λ'_{22} are functions of the transverse crack spacing, the delamination length and the in situ constraining conditions of the 90°-ply. The substitution of $l = 0$ into eqns (50a,b) gives the stiffness reduction due to a pure matrix cracking. The complete damage of the 90°-plies ($\Lambda_{22} = 1$) is approached when full delamination ($l = s$) or extremely dense transverse cracking ($l = 0$ and $s \to 0$) occur.

6. Strain energy release rate (SERR)

The potential energy method has been presented by Zhang et al. (1992b, 1994) for the evaluation of the energy release rate due to transverse ply cracking and its induced delamination. The potential energy (PE) of a damaged laminate element with a finite gauge length of $2s$ and unity width under the condition of plane strain in width-direction is

$$PE = U - N\varepsilon_y 2s \tag{51}$$

where U is the total strain energy stored in a laminate element. It is a function of the matrix cracking density and of the local delamination length. The value of the strain energy can be calculated by using the microstress field obtained in the previous sections and by integrating the strain energy density over the element, but that procedure involves tedious integration operations. An alternate way presented by Zhang et al. (1992b, 1994) is that the reduced stiffness of the constrained 90°-plies and the laminate plate theory are applied to the "equivalent" damaged laminate for computing the value of the total strain energy. For the laminate examined here without taking into account the contribution of residual hygrothermal stresses, this value is given by

$$U = sA_{22}^{\mathrm{d}}\varepsilon_y^2 \tag{52}$$

In fracture mechanics, the energy release associated with a particular damage mode is by definition equal to the first partial derivative of the potential energy with respect to the crack surface area of the respective damage; the applied laminate loads, $\{N\}$, are fixed and the other damage modes remain unchanged. Combining eqns (51), (52) and (49a), the expressions for the strain energy release rates associated with a local delamination and matrix cracking are obtained as

$$G^{\mathrm{ld}} = \frac{Q_{22}h^{(3)}s}{2}\varepsilon_y^2\frac{\partial\Lambda_{22}}{\partial l} \tag{53a}$$

$$G^{\mathrm{mc}} = -\varepsilon_y^2 Q_{22}s^2\frac{\partial\Lambda_{22}}{\partial s} \tag{53b}$$

The strain energy release rates normalized by the square of the laminate strain are

$$\frac{G^{\mathrm{ld}}}{\varepsilon_y^2} = \frac{Q_{22}h^{(3)}s}{2}\frac{\Lambda_{22}}{\partial l} \tag{54a}$$

$$\frac{G^{\mathrm{mc}}}{\varepsilon_y^2} = -Q_{22}s^2\frac{\partial\Lambda_{22}}{\partial s} \tag{54b}$$

The parameters Q_{22} and $h^{(3)}$ in eqns (53a)–(54b) are the transverse in-plane stiffness of an intact lamina and the half-thickness of the 90°-ply group, respectively. The expressions for the energy release rates vary linearly with the first derivatives of the IDEF with respect to the delamination length and the matrix crack spacing, respectively. They are valid for both the five-layer and the three-layer model laminates by utilizing corresponding IDEF expressions given by eqns (50a) and (50b).

7. Results and discussion

The T300/934 graphite/epoxy composite material system is examined here. The basic properties of a composite lamina are given by

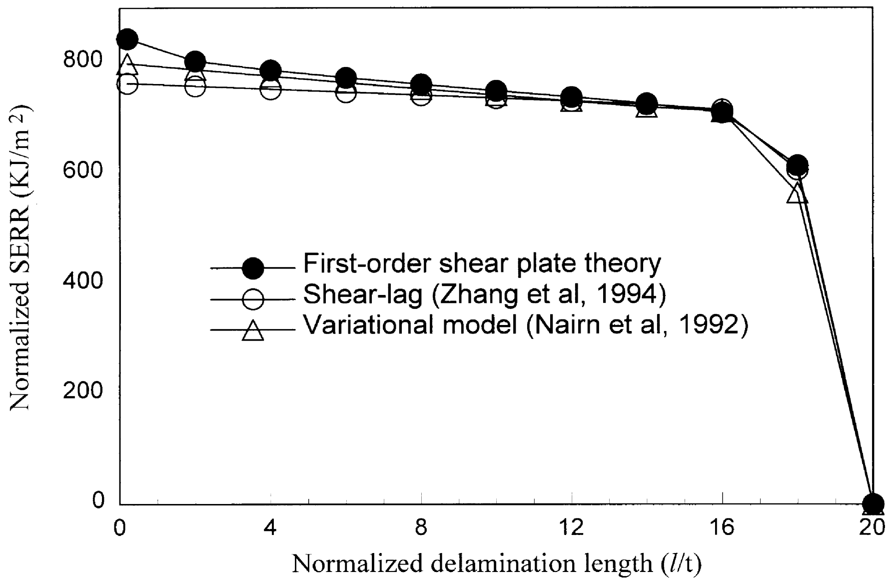

Fig. 3. A comparison between the first-order shear plate theory, the modified shear-lag model (Zhang et al., 1994) and the variational model (Nairn and Hu, 1992) in terms of the strain energy release rate associated with a local delamination in the $[0/90]_s$ laminate.

$$E_{11} = 144.8\,\text{GPa} \quad E_{22} = E_{33} = 11.38\,\text{GPa} \quad G_{12} = G_{13} = 6.48\,\text{GPa}$$

$$G_{23} = 3.45\,\text{GPa} \quad \nu_{12} = \nu_{13} = 0.3 \quad \text{single-ply thickness } t = 0.132\,\text{mm}$$

Firstly, the first-order shear deformation plate theory is compared with the Narin–Hu's (1992) variational mechanics approach and our previous modified shear-lag analysis (Zhang et al., 1992a, 1994) where the out-of-plane shear stresses are assumed to vary linearly across the thickness of the cracked ply group and constraining layers (i.e. a parabolic variation of the in-plane displacements). The $[0/90]_s$ lay-up is chosen to conduct the comparison since the variational approach and the modified shear-lag model are based on a three-layer model. In Fig. 3 the normalized SERRs for a delamination at the 0°/90° interface in the $[0/90]_s$ laminate calculated by the three models just mentioned, are plotted against the normalized delamination length. The good agreement between the models suggests that the first-order plate theory provide an accurate prediction comparable with the variational method and the modified shear-lag analysis even if a further improvement is expected to be achieved by utilizing a higher order plate theory.

7.1. *Stiffness reduction*

In this section, the stiffness reduction is examined for various lay-up laminates by calculating IDEF (Λ_{22}) as a function of the delamination length with a given transverse ply crack half-spacing of 2.64 mm which corresponds to a matrix crack density $C_d = 1.894\ \text{cm}^{-1}$. In order to identify the influences of the primary constraining layer, the nearest-neighboring orientation angle of the core 90°-ply group is allowed to vary from 0–75° and the rest constraining plies remain unchanged. In

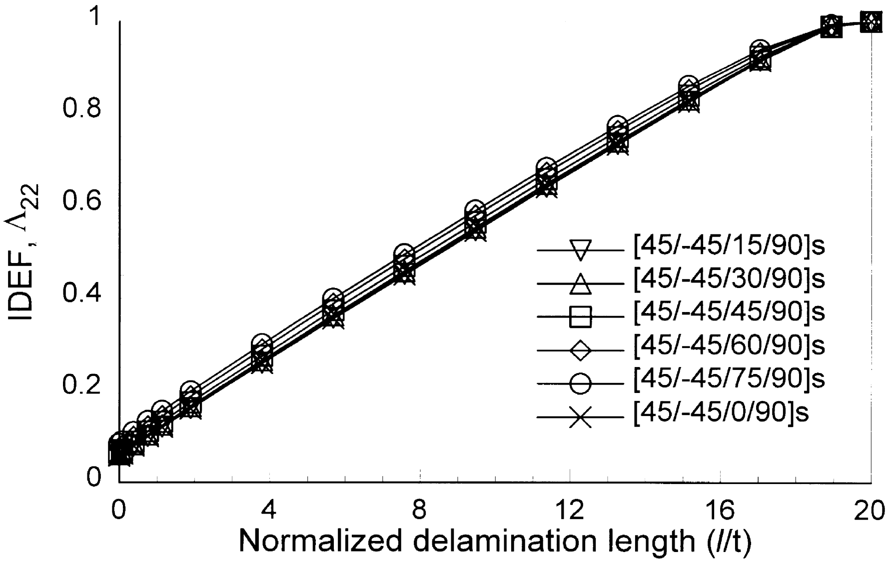

Fig. 4. IDEF as a function of the normalized delamination length for the laminates with varying primary constraining layers ($s = 2.64$ mm $= 20t$).

Fig. 4, the IDEF, Λ_{22}, calculated by the FLM is plotted vs the normalized local delamination length, l/t, for $[\pm 45/\phi/90]_s$ laminates where $\phi = 0°$, $15°$, ... and $75°$. The values of the IDEF for the all lay-ups increase (extension stiffness decreases) with increasing delamination length and reach unity when total delamination occurs ($l = s = 20t = 2.64$ mm). The curve corresponding to a bigger orientation angle ϕ lies above that associated with a smaller orientation angle; suggesting that the constraint of the primary constraining layers on the 90°-plies decreases with an increasing lay-up orientation angle. Figure 5 is a bar chart showing the effect of a changing orientation angle ϕ on IDEF when $l = 0.5$ mm. The difference of the IDEF between $\phi = 0°$ and $\phi = 75°$ is about 14%.

Figure 6 is a plot of the IDEF against the normalized local delamination length for [0/90] and $[\pm\varphi/0/90]_s$ laminates where $\varphi = 30$, 45 and 60°. It should be mentioned that the values of the IDEF for a $[0/90]_s$ laminate are calculated by the three-layer model laminate I (TLM I) which can be considered as a special case without secondary constraining layers. There is no apparent discrepancy between the different secondary constraining layers for all delamination lengths. Figure 7 is a bar chart of the IDEF against the type of a secondary constraining layer for $l = 0.5$ mm. The difference between the laminates with a stronger secondary constraining layer ($[\pm 30/0/90]_s$ laminate) and without a secondary constraining layer ($[0/90]_s$ laminate) is only 1.3% which can be ignored; suggesting that the influence of a secondary constraining layer on the stiffness reduction is negligible for the lay-ups examined here.

In Fig. 8, IDEF's calculated by both the TLM laminate II and the FLM are plotted vs the normalized delamination length for a laminate $[\pm 60/0/90]_s$. No notable difference between the two methods is seen. It is implied that a local lay-up configuration has no significant influence on a stiffness reduction.

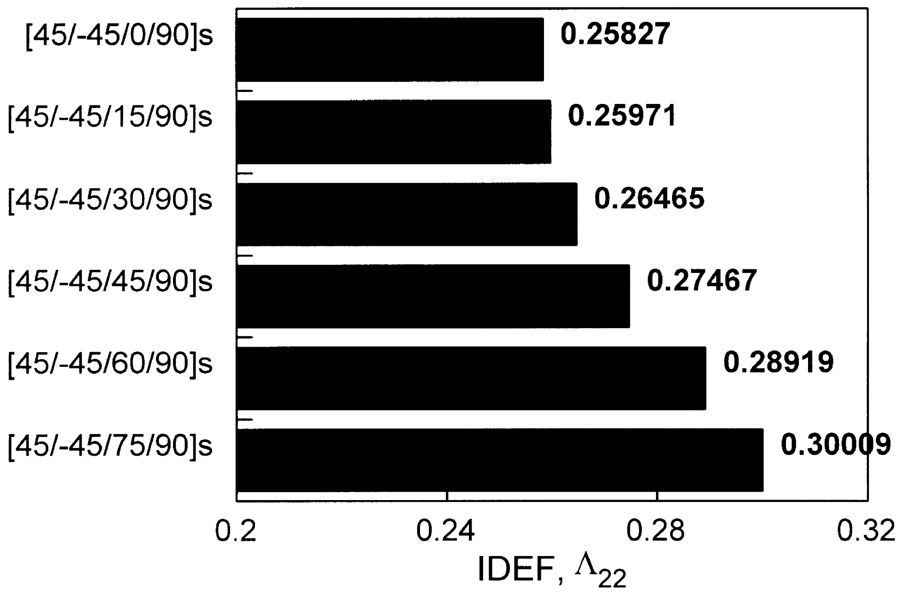

Fig. 5. IDEF varies with a changing fiber orientation of the primary constraining layer when $s = 2.64$ mm $= 20t$ and $l = 0.5$ mm.

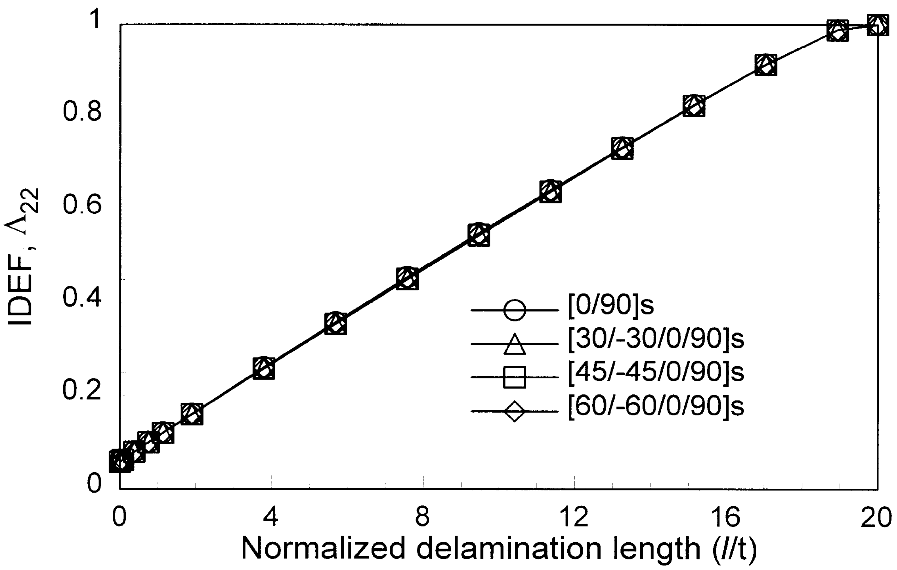

Fig. 6. IDEF as a function of the normalized delamination length for the laminates with different secondary constraining layers ($s = 2.64$ mm $= 20t$).

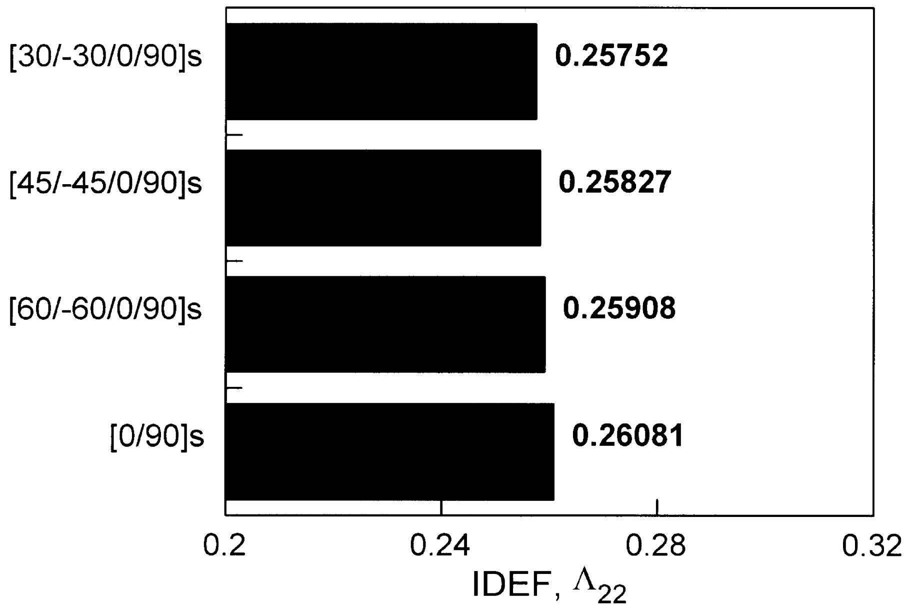

Fig. 7. Effect of the secondary constraining layer on IDEF for $s = 2.64$ mm $= 20t$ and $l = 0.5$ mm.

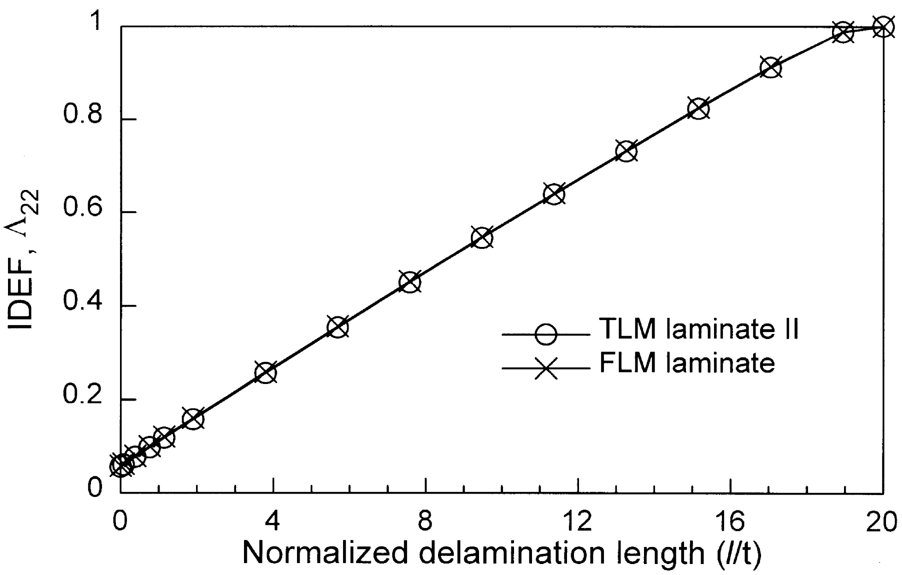

Fig. 8. IDEF predicted by the FLM laminate and the TLM II laminate as a function of the normalized delamination length for the $[\pm 60/0/90]_s$ laminate.

Therefore, one could conclude that the TLM laminate I of $[\phi_m/90_{2n}/\phi_m]_T$, the TLM laminate II $[S'^L/90_{2n}/S'^R]_T$ and the FLM laminate $[S^L/\phi_m/90_{2n}/\phi_m/S^R]_T$, where S^L, S^R, S'^L and S'^R are sub-laminates $[\ldots/\varphi_i]_T$, $[\varphi_i/\ldots]_T$, $[\ldots/\varphi_i/\phi_m]_T$ and $[\phi_m/\varphi_i/\ldots]_T$, respectively, result in a comparable accuracy for modeling the reduced stiffness of the 90°-plies in $[\ldots/\varphi_i/\phi_m/90_n]_s$ under in situ constraining conditions. Consequently, the more simple TLM laminate I $[\phi_m/90_{2n}/\phi_m]_T$ consisting of the 90°-plies and their next neighboring orientation ply groups could be used to analyze the stiffness reduction of the constrained 90°-plies in $[\ldots/\varphi_i/\phi_m/90_n]_s$ laminates.

7.2. *Strain energy release rate* (*SERR*)

The normalized strain energy release rate for a local delamination is proportional to the first partial derivative of the IDEF with respect to the delamination length, $\partial\Lambda_{22}/\partial l$, [see eqn (54a)] which can be evaluated with the three model laminates, respectively. Assuming a constant transverse crack density $C_d = 1.894\ \mathrm{cm}^{-1}$ (transverse matrix crack half-spacing $s = 20t = 2.64$ mm) the normalized strain energy release rate is plotted against the normalized delamination length, l/t, for various laminate stacking sequences.

Figures 9–12 show the comparison between the FLM $[S^L/\phi_m/90_{2n}/\phi_m/S^R]_t$ laminate and the TLM II $[S'^R/90_{2n}/S'^L]_T$ laminate for four laminates $[\pm\varphi/0/90]_s$ ($\varphi = 30$, 45, 60°) and $[0/\pm 45/90]_s$. The two models agree well when the delamination length exceeds about two single-ply thicknesses for laminates $[\pm\varphi/0/90]_s$ ($\varphi = 30, 45, 60°$) and about one single-ply thickness for a $[0/\pm 45/90]_s$ laminate. For a shorter delamination length the more accurate FLM laminate predicts a notably bigger SERR than the TLM II laminate. It is suggested that the strain energy release rate for a delamination, unlike the stiffness reduction, largely depends upon the details of a local lay-up configuration of a damaged laminate.

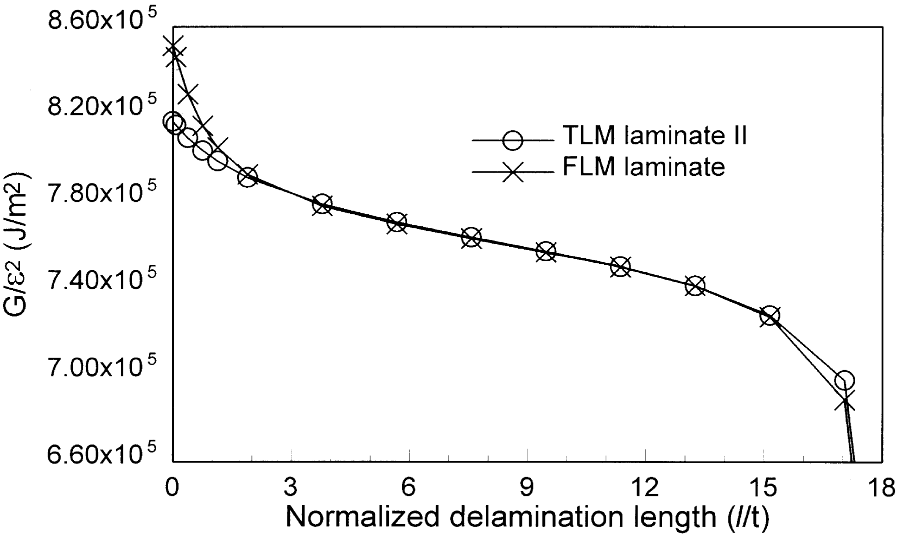

Fig. 9. Normalized strain energy release rate for a local delamination predicted by the FLM laminate and the TLM II laminate as a function of the normalized delamination length for the $[\pm 30/0/90]_s$ laminate ($s = 2.64$ mm $= 20t$).

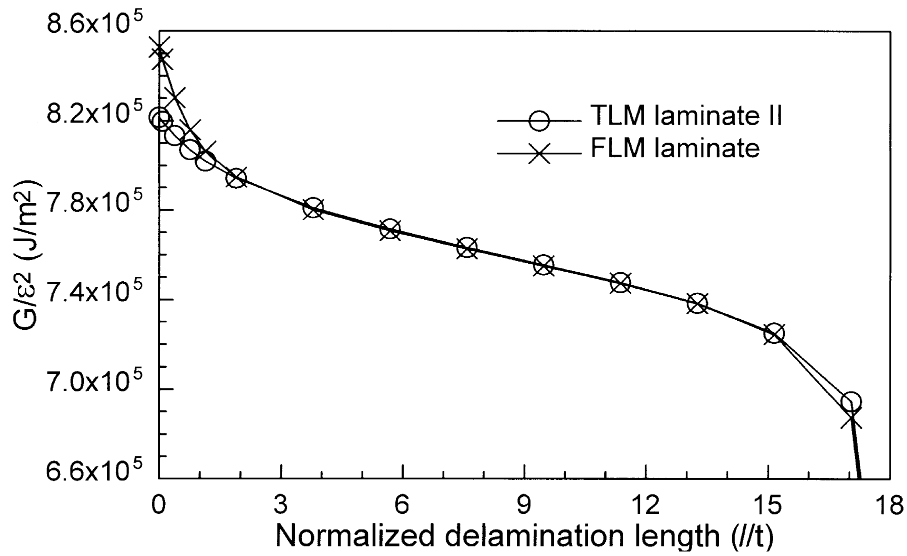

Fig. 10. Normalized strain energy release rate for a local delamination predicted by the FLM laminate and the TLM II laminate as a function of the normalized delamination length for the $[\pm 45/0/90]_s$ laminate ($s = 2.64$ mm $= 20t$).

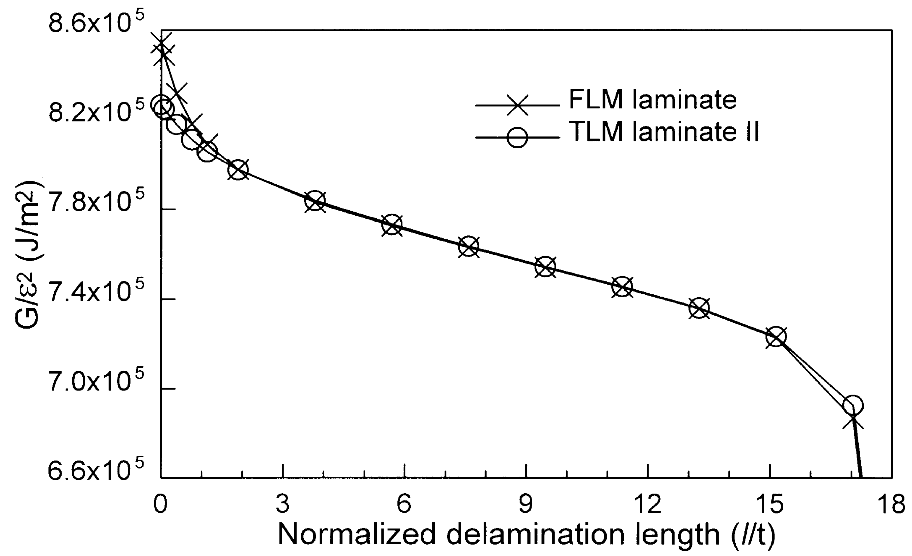

Fig. 11. Normalized strain energy release rate for a local delamination predicted by the FLM laminate and the TLM II laminate as a function of the normalized delamination length for the $[\pm 60/0/90]_s$ laminate ($s = 2.64$ mm $= 20t$).

Figure 13 presents predictions of the FLM for laminates $[\pm 45/\phi/90]_s$ with various primary constraining ply orientations and the same secondary constraining layer. The SERRs increase considerably with an increasing orientation angle of the next neighboring ply of the core 90°-plies.

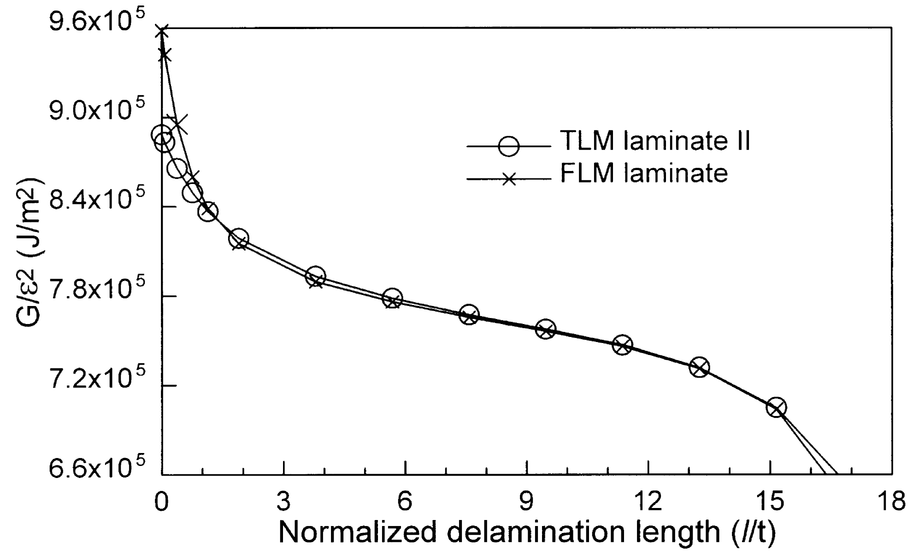

Fig. 12. Normalized strain energy release rate for a local delamination predicted by the FLM laminate and the TLM II laminate as a function of the normalized delamination length for the $[0/\pm45/90]_s$ laminate ($s = 2.64$ mm $= 20t$).

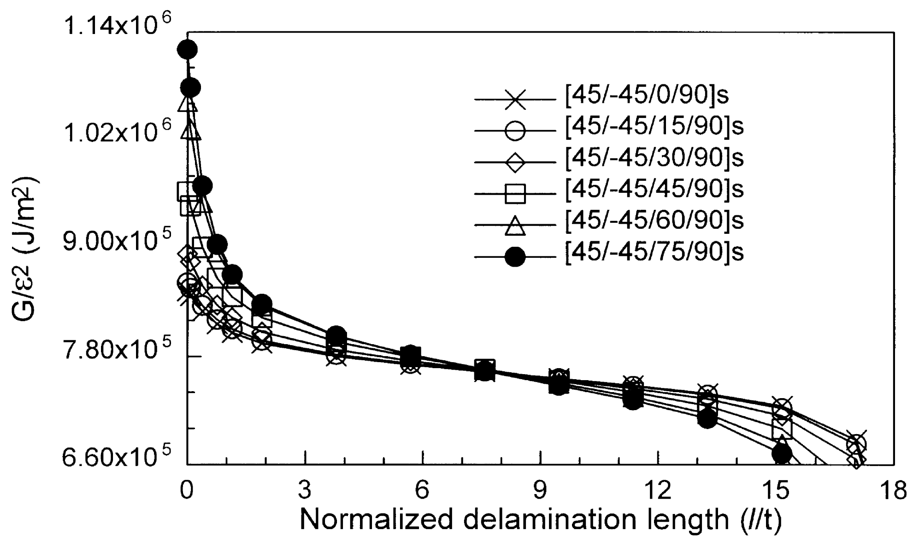

Fig. 13. Effect of the primary constraining layer on the normalized strain energy release rate for a local delamination predicted by the FLM laminate for the $[45/\phi/90]_s$ laminates ($s = 2.64$ mm $= 20t$).

In order to examine the effect of a secondary constraining layer on the SERR the laminates with the same primary constraining layer and varying rest constraining plies are used in Fig. 14. The values of the SERR for all examined laminates with the secondary constraining layers varying

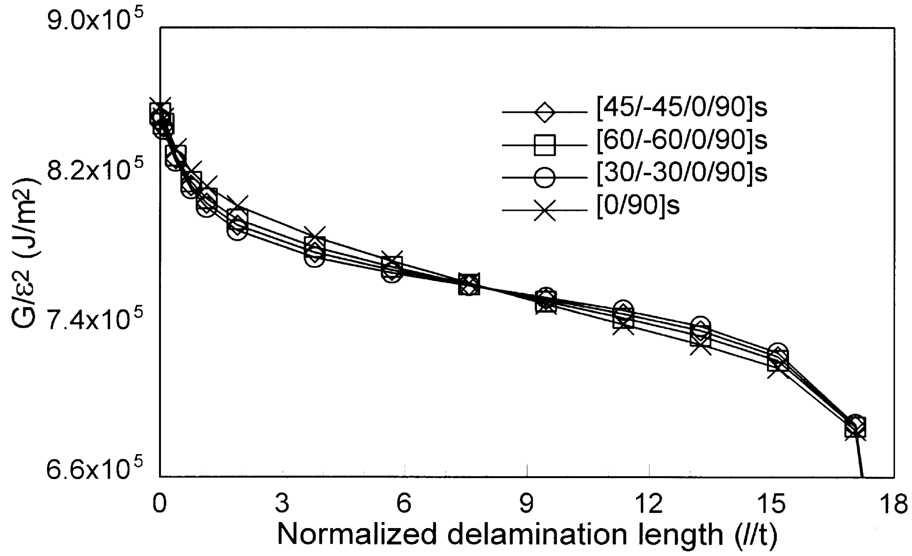

Fig. 14. Effects of the secondary constraining layer on the normalized strain energy release rate for a local delamination predicted by the FLM laminate ($s = 2.64$ mm $= 20t$).

from [± 30], [± 45] and [± 60] and without a secondary constraining layer are in a good agreement, suggesting that the secondary constraining layers can be ignored for the evaluation of the normalized SERR for the examined laminates. Again, the more simple TLM II $[\phi_m/90_{2n}/\phi_m]_T$ laminate consisting of the 90°-plies and their next neighboring ply groups can be used to analyze the strain energy release rate for a local delamination at the $\phi/90°$ interface in $[\ldots/\varphi_i/\phi_m/90_n]_s$ laminates by applying the same laminate strain to both of the two laminates.

8. Concluding remarks

Local delaminations initiating and growing from transverse ply cracks in $[\ldots/\varphi_i/\phi_m/90_n]_s$ laminates were studied by using a first-order shear laminate theory. The three model laminates, a five-layer model (FLM) $[S^L/\phi_m/90_{2n}/\phi_m/S^R]_T$, and two three-layer model (TLM) laminates, $[\phi_m/90_{2n}/\phi_m]_T$ and $[S'^L/90_{2n}/S'^R]_T$, were proposed to examine constraining mechanisms of the constraining plies of the center 90°-ply group on transverse crack induced delaminations, where S^L, S^R, S'^L and S'^R are sublaminates $[\ldots/\varphi_i]_T$, $[\varphi_i/\ldots]_T$, $[\ldots/\varphi_i/\phi_m]_T$ and $[\phi_m/\varphi_i/\ldots]_T$, respectively. The microstress and microstrain fields in the cracked and delaminated five-layer and three-layer model laminates were obtained by using the first-order shear laminate theory.The explicit expression for the stiffness reduction of the constrained 90°-plies was derived as a function of delamination length and transverse crack spacing. The strain energy release rates associated with a local delamination and matrix cracking vary linearly with the first derivatives of the IDEF with respect to the delamination length and crack spacing, respectively. It was seen for the examined laminates that the nearest neighboring ply group of the 90°-plies primarily affects the stiffness reduction of the constrained transverse plies and also the normalized strain energy release rate whereas the influences of the other constraining layers are ignorable. The strain energy release rate for a local delamination largely depends on a local lay-up configuration of a damaged laminate but the stiffness reduction does not. Consequently, the three-layer model laminate, consisting of the 90°-ply group and its two next neighboring ply groups, could be used to analyze the in situ reduced stiffness of the constrained transverse plies and the strain energy release rates due to a delamination and matrix cracking in the $[\ldots/\varphi_i/\phi_m/90_n]_s$ laminates. Therefore, a more complicated ply-by-ply analysis for a complete laminate is not needed.

Acknowledgements

This work was financially supported by the State Education Commission of China, the National Science Foundation of China and the Alexander von Humboldt-Foundation of Germany.

Appendix 1. Derivation of the governing eqn (7)

The symmetry of the laminate implies

$$T_{\rm b}^{(3)} = 0 \tag{A1.1}$$

The load-free condition at the top surface of the laminate and the reciprocal tractions at the interfaces between the sublaminates can be specified as

$$T_{\rm t}^{(1)} = 0 \quad T_{\rm b}^{(1)} = T_{\rm t}^{(2)} \quad T_{\rm b}^{(2)} = T_{\rm t}^{(3)} \tag{A1.2a,b,c}$$

$$P_{\rm t}^{(1)} = 0 \quad P_{\rm b}^{(1)} = P_{\rm t}^{(2)} \quad P_{\rm b}^{(2)} = P_{\rm t}^{(3)} \tag{A1.2d,e,f}$$

The second derivatives of eqns (5a,b) with respect to y read

$$V_{,yy}^{(1)} - \frac{h^{(1)}}{2}\beta_{,yy}^{(1)} = V_{,yy}^{(2)} + \frac{h^{(2)}}{2}\beta_{,yy}^{(2)} \tag{A1.3a}$$

$$V_{,yy}^{(2)} - \frac{h^{(2)}}{2}\beta_{,yy}^{(2)} = V_{,yy}^{(3)} + \frac{h^{(3)}}{2}\beta_{,yy}^{(3)} \tag{A1.3b}$$

Combination of eqns (6a–c), (A1.3a,b) and (A1.2b,c) leads to

$$T_{\rm b}^{(1)} = T_{\rm t}^{(2)} = \frac{1}{A_{22}}[(A_{22}^{(2)} + A_{22}^{(3)})(2B_{22}^{(1)} + h^{(1)}A_{22}^{(1)})\beta_{,yy}^{(1)} + h^{(2)}A_{22}^{(1)}(A_{22}^{(2)} + 2A_{22}^{(3)})\beta_{,yy}^{(2)} + h^{(3)}A_{22}^{(1)}A_{22}^{(3)}\beta_{,yy}^{(3)}] \tag{A1.4a}$$

$$T_{\rm b}^{(2)} = T_{\rm t}^{(3)} = \frac{A_{22}^{(3)}}{A_{22}}[(2B_{22}^{(1)} + h^{(1)}A_{22}^{(1)})\beta_{,yy}^{(1)} + h^{(2)}(A_{22}^{(2)} + 2A_{22}^{(1)})\beta_{,yy}^{(2)} + h^{(3)}(A_{22}^{(1)} + A_{22}^{(2)})\beta_{,yy}^{(3)}] \tag{A1.4b}$$

$$V^{(1)}_{,yy} = \frac{1}{A_{22}}[(h^{(1)}(A^{(2)}_{22}+A^{(3)}_{22})-2B^{(1)}_{22})\beta^{(1)}_{,yy}+h^{(2)}(A^{(2)}_{22}+2A^{(3)}_{22})\beta^{(2)}_{,yy}+h^{(3)}A^{(3)}_{22}\beta^{(3)}_{,yy}] \tag{A1.4c}$$

$$V^{(2)}_{,yy} = \frac{-1}{A_{22}}[(h^{(1)}A^{(1)}_{22}+2B^{(1)}_{22})\beta^{(1)}_{,yy}+h^{(2)}(A^{(1)}_{22}-A^{(3)}_{22})\beta^{(2)}_{,yy}-h^{(3)}A^{(3)}_{22}\beta^{(3)}_{,yy}] \tag{A1.4d}$$

$$V^{(3)}_{,yy} = \frac{-1}{A_{22}}[(h^{(1)}A^{(1)}_{22}+2B^{(1)}_{22})\beta^{(1)}_{,yy}+h^{(2)}(2A^{(1)}_{22}+A^{(2)}_{22})\beta^{(2)}_{,yy}+h^{(3)}(A^{(1)}_{22}+A^{(2)}_{22})\beta^{(3)}_{,yy}] \tag{A1.4e}$$

where A_{22} is the extension stiffness of an intact laminate (see Appendix 3). The substitution of eqns (A1.4a,b,c) into eqns (6d–f) gives the governing eqn (7). By integrating equation (A1.4c–e) and by eliminating the rigid body displacements give

$$V^{(1)} = \frac{1}{A_{22}}[(h^{(1)}(A^{(2)}_{22}+A^{(3)}_{22})-2B^{(1)}_{22})\beta^{(1)}+h^{(2)}(A^{(2)}_{22}+2A^{(3)}_{22})\beta^{(2)}+h^{(3)}A^{(3)}_{22}\beta^{(3)}]+\alpha_4 y \tag{A1.5a}$$

$$V^{(2)} = \frac{-1}{A_{22}}[(h^{(1)}A^{(1)}_{22}+2B^{(1)}_{22})\beta^{(1)}+h^{(2)}(A^{(1)}_{22}-A^{(3)}_{22})\beta^{(2)}-h^{(3)}A^{(3)}_{22}\beta^{(3)}]+\alpha_5 y \tag{A1.5b}$$

$$V^{(3)} = \frac{-1}{A_{22}}[(h^{(1)}A^{(1)}_{22}+2B^{(1)}_{22})\beta^{(1)}+h^{(2)}(2A^{(1)}_{22}+A^{(2)}_{22})\beta^{(2)}+h^{(3)}(A^{(1)}_{22}+A^{(2)}_{22})\beta^{(3)}]+\alpha_6 y \tag{A1.5c}$$

Appendix 2. Determination of the constants α_i, θ_j and ψ_k

The substitution of eqns (12), (22), (24a,b), (25a,b) and (29a) into the boundary conditions for the sublaminates, eqns (30a–f), give

$$\psi_3 = 0 \tag{A2.1a}$$

$$q(\theta_1 e^{\omega s}+\theta_2 e^{-\omega s})+\theta_3 s+\theta_4 = 0 \tag{A2.1b}$$

$$\theta_1 e^{\omega s}+\theta_2 e^{-\omega s}+\theta_3 s+\theta_4 = 0 \tag{A2.1c}$$

$$\tfrac{1}{2}(h^{(2)}q+h^{(1)})(\theta_2 e^{\omega s}+\theta_2 e^{-\omega s})+(\theta_6-\theta_5)s+\theta_8-\theta_7 = 0 \tag{A2.1d}$$

$$A^{(2)}_{22}\theta_5+A^{(1)}_{22}\theta_6+B^{(1)}_{22}\theta_3 = \tfrac{1}{2}N \tag{A2.1e}$$

$$A^{(1)}_{22}\alpha_4+A^{(2)}_{22}\alpha_5+A^{(3)}_{22}\alpha_6 = \tfrac{1}{2}N \tag{A2.1f}$$

Substituting eqns (10, 11) into the interfacial continuity conditions, eqns (5a,b), one can obtain

$$\alpha_4 = \alpha_5 \quad \alpha_5 = \alpha_6 \tag{A2.2a,b}$$

Furthermore, the continuity relations (31a–k) take the form

$$\sum_{j=1}^{3}\alpha_j\gamma^{(1)}_j \sinh(\lambda_j(s-l))+\alpha_4(s-l) = k_3(\theta_1 e^{\omega(s-l)}+\theta_2 e^{\omega(s-1)})+\theta_6(s-l)+\theta_8 \tag{A2.2c}$$

$$\sum_{j=1}^{3} \alpha_j \gamma_j^{(2)} \sinh(\lambda_j(s-l)) + \alpha_5(s-l) = -k_1(\theta_1\, e^{\omega(s-l)} + \theta_2\, e^{-\omega(s-l)}) + \theta_5(s-l) + \theta_7 \tag{A2.2d}$$

$$\sum_{j=1}^{3} \alpha_j \gamma_j^{(3)} \sinh(\lambda_j(s-l)) + \alpha_6(s-l) = \psi_4 \tag{A2.2e}$$

$$\sum_{j=1}^{3} \alpha_j p_j^{(1)} \sinh(\lambda_j(s-l)) = \theta_1\, e^{\omega(s-l)} + \theta_2\, e^{-\omega(s-l)} + \theta_3(s-l) + \theta_4 \tag{A2.2f}$$

$$\sum_{j=1}^{3} \alpha_j p_j^{(2)} \sin(\lambda_j(s-l)) = q(\theta_1\, e^{\omega(s-l)} + \theta_2\, e^{-\omega(s-l)}) + \theta_3(s-l) + \theta_4 \tag{A2.2g}$$

$$\sum_{j=1}^{3} \alpha_j \sinh(\lambda_j(s-l)) = \psi_1\, e^{\omega_1(s-1)} + \psi_2\, e^{-\omega_1(s-l)} \tag{A2.2h}$$

$$-\frac{A_{44}^{(1)} + A_{44}^{(2)} q}{\omega(A_{44}^{(1)} + A_{44}^{(2)})}(\theta_1\, e^{\omega(s-1)} - \theta_2\, e^{-\omega(s-l)}) - \frac{1}{2}\theta_3(s-l)^2 - \theta_4(s-l) + \theta_9 = 0 \tag{A2.2i}$$

$$\sum_{j=1}^{3} \alpha_j \eta_j^{(2)} \cosh(\lambda_j(s-l)) + A_{22}^{(2)}\alpha_4 = -k_1\omega A_{22}^{(2)}(\theta_1\, e^{\omega(s-l)} - \theta_2\, e^{-\omega(s-l)}) + A_{22}^{(2)}\theta_5 \tag{A2.2j}$$

$$\sum_{j=1}^{3} \alpha_j \eta_j^{(3)} \cosh(\lambda_j(s-l)) + A_{22}^{(3)}\alpha_6 = 0 \tag{A2.2k}$$

$$\sum_{j=1}^{3} \alpha_j p_j^{(2)} \lambda_j \cosh(\lambda_j(s-l)) = \omega q(\theta_1\, e^{\omega(s-l)} - \theta_2\, e^{-\omega(s-l)}) + \theta_3 \tag{A2.2l}$$

$$\sum_{j=1}^{3} \alpha_j \lambda_j \cosh(\lambda_j(s-l)) = \omega_1(\psi_1\, e^{\omega_1(s-l)} - \psi_2\, e^{-\omega_1(s-l)}) \tag{A2.2m}$$

The subtraction of eqn (A2.1c) from eqn (A2.1b) gives

$$\theta_2 = -\theta_1\, e^{2\omega s} \tag{A2.3}$$

Substituting eqn (A2.3) into eqn (A2.1c,d) results in

$$\theta_4 = -\theta_3 s \tag{A2.4}$$

$$(\theta_6 - \theta_5)s + \theta_8 - \theta_7 = 0 \tag{A2.5}$$

The subtraction of eqn (A2.2d) from eqn (A2.2c) gives the result

$$\frac{1}{2}\sum_{j=1}^{3} \alpha_j (h^{(1)} p_j^{(1)} + h^{(2)} p_j^{(2)}) \sinh(\lambda_j(s-l)) = \frac{1}{2}(h^{(2)} q + h^{(1)})(\theta_1\, e^{\omega(s-l)} + \theta_2\, e^{-\omega(s-l)}) - (\theta_6 - \theta_5) l \tag{A2.6a}$$

An appropriate combination of eqns (A2.2f) and (A2.2g) gives

$$\sum_{j=1}^{3} \alpha_j (h^{(1)} p_j^{(1)} + h^{(2)} p_j^{(2)}) \sinh(\lambda_j (s-l))$$

$$= (h^{(2)} q + h^{(1)})(\theta_1 \, e^{\omega(s-l)} + \theta_2 \, e^{-\omega(s-l)}) - (h^{(1)} + h^{(2)})\theta_3 l \quad \text{(A2.6b)}$$

The subtraction of eqn (A2.2g) from eqn (A2.2f) reads as follows

$$\sum_{j=1}^{3} \alpha_j (p_j^{(1)} - p_j^{(2)}) \sinh(\lambda_j (s-l)) = 2\theta_1 (\mathrm{q}-1) \, \mathrm{e}^{\omega s} \sinh(\omega l) \quad \text{(A2.6c)}$$

A further combination of eqns (A2.2f) and (A2.2g) gives

$$\sum_{j=1}^{3} \alpha_j (p_j^{(1)} q - p_j^{(2)}) \sinh(\lambda_j (s-l)) = \theta_3 (1-q) l \quad \text{(A2.6d)}$$

Moreover, from eqns (A2.6a) and (A2.6b) follows

$$[2\theta_6 - 2\theta_5 - (h^{(1)} + h^{(2)})\theta_3] l = 0 \quad \text{(A2.7)}$$

Using eqns (A2.7) and (A2.1e) one arrives at

$$\theta_5 = \frac{N}{2(A_{22}^{(1)} + A_{22}^{(2)})} - \theta_3 k_5 \quad \theta_6 = \frac{N}{2(A_{22}^{(1)} + A_{22}^{(2)})} + \theta_3 k_4 \quad \text{(A2.8a,b)}$$

where k_4 and k_5 are listed in Appendix 3. The substitution of eqns (A2.2a) and (A2.2b) into eqn (A2.1f) gives eqn (32b), i.e.

$$\alpha_4 = \alpha_5 = \alpha_6 = \frac{N}{A_{22}} \quad \text{(A2.9)}$$

Eqns (A2.2j) and (A2.2) can be re-written as follows by using eqns (A2.3), (A2.9), (A2.8a) and (A2.8b)

$$\sum_{j=1}^{3} \alpha_j \gamma_j^{(2)} \lambda_j \cosh(\lambda_j (s-l)) - \frac{\chi N}{A_{22}} = -2k_1 \omega \, e^{\omega s} \cosh(\omega l)\theta_1 - k_5 \theta_3 \quad \text{(A2.10a)}$$

$$\sum_{j=1}^{3} \alpha_j p_j^{(2)} \lambda_j \cosh(\lambda_j (s-l)) = 2\omega q \, e^{\omega s} \cosh(\omega l)\theta_1 + \theta_3 \quad \text{(A2.10b)}$$

The solutions of the above two equations read

$$\theta_3 = \sum_{j=1}^{3} \alpha_j \delta_j \cosh(\lambda_j (s-l)) + \frac{k_6}{A_{22}} N \quad \text{(A2.11a)}$$

$$e^{\omega s} \cosh(\omega l)\theta_1 = \sum_{j=1}^{3} \alpha_j \rho_j \cosh(\lambda_j (s-l)) + \frac{k_7}{A_{22}} N \quad \text{(A2.11b)}$$

where k_6, k_7, δ_j and ρ_j are given in Appendix 3. The substitution of eqns (A2.11a,b) into eqns (A2.6c,d) and of eqn (A2.9) into eqn (A2.2k) gives

$$\sum_{j=1}^{3}\alpha_j[(p_j^{(1)}-p_j^{(2)})\sinh(\lambda_j(s-l))+2(1-q)\rho_j\tanh(\omega l)\cosh(\lambda_j(s-l))]$$

$$=-2(1-q)k_7\tanh(\omega l)\frac{N}{A_{22}} \quad \text{(A2.12a)}$$

$$\sum_{j=1}^{3}\alpha_j[(p_j^{(1)}q-p_j^{(2)})\sinh(\lambda_j(s-l))-(1-q)\delta_j l\cosh(\lambda_j(s-l))]=(1-q)k_6 l\frac{N}{A_{22}} \quad \text{(A2.12b)}$$

$$\sum_{j=1}^{3}\alpha_j\eta_j^{(3)}\cosh(\lambda_j(s-l))=-\frac{A_{22}^{(3)}}{A_{22}}N \quad \text{(A2.12c)}$$

Eqn (32a) is obtained when these three equations are written in the form of a matrix. Further, the substitution of eqns (A2.8a,b) into eqns (A2.2c,d) gives

$$\theta_5 s+\theta_7=\frac{N}{A_{22}}(s+\chi l)-k_5 l\theta_3+\sum_{j=1}^{3}\alpha_j\gamma_j^{(2)}\sinh(\lambda_j(s-l))-2\theta_1 k_1 e^{\omega s}\sinh(\omega l) \quad \text{(A2.13a)}$$

$$\theta_6 s+\theta_8=\frac{N}{A_{22}}(s+\chi l)+k_4 l\theta_3+\sum_{j=1}^{3}\alpha_j\gamma_j^{(1)}\sinh(\lambda_j(s-l))+2\theta_1 k_3 e^{\omega s}\sinh(\omega l) \quad \text{(A2.13b)}$$

By using eqns (A2.6c,d), eqn (A2.13a,b) can be further reduced to

$$\theta_5 s+\theta_7=\frac{N}{A_{22}}\left[s+\chi\left(l+\sum_{j=1}^{3}\bar{\alpha}_j\gamma_j^{(3)}\tanh(\lambda_j(s-l))\right)\right] \quad \text{(A2.13c)}$$

$$\theta_6 s+\theta_8=\frac{N}{A_{22}}\left[s+\chi\left(l+\sum_{j=1}^{3}\bar{\alpha}_j\gamma_j^{(3)}\tanh(\lambda_j(s-l))\right)\right] \quad \text{(A2.13d)}$$

The substitution of eqns (A2.3) and (A2.4) into eqn (A2.2i) gives

$$\theta_9=\frac{2(A_{44}^{(1)}+A_{44}^{(2)}q)}{\omega(A_{44}^{(1)}+A_{44}^{(2)})}\theta_1 e^{\omega s}\cosh(\omega l)-\frac{1}{2}\theta_3(s^2-l^2) \quad \text{(A2.13e)}$$

Moreover, ψ_1, ψ_2 and ψ_4 can be expressed by solving eqns (A2.2e,h,m)

$$\psi_1=\frac{1}{2\omega_1}e^{-\omega_1(s-l)}\sum_{j=1}^{3}\alpha_j[\omega_1\sinh(\lambda_j(s-l))+\lambda_j\cosh(\lambda_j(s-l))] \quad \text{(A2.14a)}$$

$$\psi_2=\frac{1}{2\omega_1}e^{\omega_1(s-l)}\sum_{j=1}^{3}\alpha_j[\omega_1\sinh(\lambda_j(s-l))-\lambda_j\cosh(\lambda_j(s-l))] \quad \text{(A2.14b)}$$

$$\psi_4=\sum_{j=1}^{3}\alpha_j\gamma_j^{(3)}\sinh(\lambda_j(s-l))+(s-l)\frac{N}{A_{22}} \quad \text{(A2.14c)}$$

Appendix 3. A list of the constants in the flm analysis

$$A_{22}=2(A_{22}^{(1)}+A_{22}^{(2)}+A_{22}^{(3)}) \quad \chi=\frac{A_{22}^{(3)}}{A_{22}^{(1)}+A_{22}^{(2)}} \quad \text{(A3.1a,b)}$$

$$a_{ij} = a_{ji} \tag{A3.2a}$$

$$a_{11} = D_{22}^{(1)} + \frac{h^{(1)}(4B_{22}^{(1)} + h^{(1)}A_{22}^{(1)})(A_{22}^{(2)} + A_{22}^{(3)}) - 4B_{22}^{(1)^2}}{2A_{22}} \tag{A3.2b}$$

$$a_{12} = \frac{h^{(2)}(B_{22}^{(1)} + \frac{1}{2}h^{(1)}A_{22}^{(1)})(A_{22}^{(2)} + 2A_{22}^{(3)})}{A_{22}} \tag{A3.2c}$$

$$a_{13} = \frac{h^{(3)}(B_{22}^{(1)} + \frac{1}{2}h^{(1)}A_{22}^{(1)})A_{22}^{(3)}}{A_{22}} \tag{A3.2d}$$

$$a_{22} = D_{22}^{(2)} + \frac{h^{(2)^2}(4A_{22}^{(1)}A_{22}^{(3)} + A_{22}^{(2)}A_{22}^{(3)} + A_{22}^{(1)}A_{22}^{(2)})}{2A_{22}} \tag{A3.2e}$$

$$a_{23} = \frac{h^{(2)}h^{(3)}A_{22}^{(3)}(A_{22}^{(2)} + 2A_{22}^{(1)})}{2A_{22}} \tag{A3.2f}$$

$$a_{33} = D_{22}^{(3)} + \frac{h^{(3)^2}A_{22}^{(3)}(A_{22}^{(2)} + A_{22}^{(1)})}{2A_{22}} \tag{A3.2g}$$

$$\eta_j^{(1)} = (B_{22}^{(1)}p_j^{(1)} + A_{22}^{(1)}\gamma_j^{(1)})\lambda_j \quad \eta_j^{(2)} = A_{22}^{(2)}\gamma_j^{(2)}\lambda_j \tag{A3.3a,b}$$

$$\eta_j^{(3)} = A_{22}^{(3)}\gamma_j^{(3)}\lambda_j = -(\eta_j^{(1)} + \eta_j^{(2)}) \quad \xi_j^{(1)} = (D_{22}^{(1)}p_j^{(1)} + B_{22}^{(1)}\gamma_j^{(1)})\lambda_j \tag{A3.3c,d}$$

$$\xi_j^{(2)} = D_{22}^{(2)}p_j^{(2)}\lambda_j \quad \xi_j^{(3)} = D_{33}^{(3)}\lambda_j \tag{A3.3e,f}$$

$$\gamma_j^{(1)} = \frac{p_j^{(1)}[h^{(1)}(A_{22}^{(2)} + A_{22}^{(3)}) - 2B_{22}^{(1)}] + p_j^{(2)}h^{(2)}(A_{22}^{(2)} + 2A_{22}^{(3)}) + h^{(3)}A_{22}^{(3)}}{A_{22}} \tag{A3.3g}$$

$$\gamma_j^{(2)} = -\frac{p_j^{(1)}(h^{(1)}A_{22}^{(1)} + 2B_{22}^{(1)}) + p_j^{(2)}h^{(2)}(A_{22}^{(1)} - A_{22}^{(3)}) - h^{(3)}A_{22}^{(3)}}{A_{22}} \tag{A3.3h}$$

$$\gamma_j^{(3)} = -\frac{p_j^{(1)}(h^{(1)}A_{22}^{(1)} + 2B_{22}^{(1)}) + p_j^{(2)}h^{(2)}(2A_{22}^{(1)} + A_{22}^{(2)}) + h^{(3)}(A_{22}^{(1)} + A_{22}^{(2)})}{A_{22}} \tag{A3.3i}$$

for $j = 1, 2, 3$

$$b_{11} = D_{22}^{(2)} + \frac{h^{(2)^2}A_{22}^{(1)}A_{22}^{(2)}}{4(A_{22}^{(1)} + A_{22}^{(2)})} \tag{A3.4a}$$

$$b_{21} = b_{12} = \frac{h^{(2)}A_{22}^{(2)}(2B_{22}^{(1)} + h^{(1)}A_{22}^{(1)})}{4(A_{22}^{(1)} + A_{22}^{(2)})} \tag{A3.4b}$$

$$b_{22} = D_{22}^{(1)} + \frac{h^{(1)}A_{22}^{(2)}(4B_{22}^{(1)} + A_{22}^{(1)}h^{(1)}) - 4B_{22}^{(1)^2}}{4(A_{22}^{(1)} + A_{22}^{(2)})} \tag{A3.4c}$$

$$k_1 = \frac{A_{22}^{(1)}(h^{(2)}q+h^{(1)})+2B_{22}^{(1)}}{2(A_{22}^{(1)}+A_{22}^{(2)})} \quad k_2 = \omega q D_{22}^{(2)} \tag{A3.5a,b}$$

$$k_3 = \frac{A_{22}^{(2)}(h^{(2)}q+h^{(1)})-2B_{22}^{(1)}}{2(A_{22}^{(1)}+A_{22}^{(2)})} \quad k_4 = \frac{(h^{(1)}+h^{(2)})A_{22}^{(2)}-2B_{22}^{(1)}}{2(A_{22}^{(1)}+A_{22}^{(2)})} \tag{A3.5c,d}$$

$$k_5 = \frac{(h^{(1)}+h^{(2)})A_{22}^{(1)}+2B_{22}^{(1)}}{2(A_{22}^{(1)}+A_{22}^{(2)})} \quad k_6 = \frac{\chi q}{k_5 q - k_1} \tag{A3.5e,f}$$

$$k_7 = -\frac{\chi}{2\omega(k_5 q - k_1)} \tag{A3.5g}$$

$$\delta_j = \frac{\lambda_j(q\gamma_j^{(2)}+k_1 p_j^{(2)})}{k_1 - k_5 q} \quad \rho_j = \frac{\lambda_j(\gamma_j^{(2)}+k_5 p_j^{(2)})}{2\omega(k_1 - k_5 q)} \tag{A3.6a,b}$$

for $j = 1, 2, 3$.

Appendix 4. A List of the constants in the TLM analysis

$$A'_{22} = 2(A'^{(1)}_{22}+A'^{(2)}_{22}) \quad \chi' = \frac{A'^{(2)}_{22}}{A'^{(1)}_{22}} \tag{A4.1a,b}$$

$$a'_{11} = D'^{(1)}_{22} + \frac{h'^{(1)}(4B'^{(1)}_{22}+h'^{(1)}A'^{(1)}_{22})A'^{(2)}_{22} - 4B'^{(1)^2}_{22}}{2A'_{22}} \tag{A4.2a}$$

$$a'_{12} = a'_{21} = \frac{h'^{(2)}(B'^{(1)}_{22}+\frac{1}{2}h'^{(1)}A'^{(1)}_{22})A'^{(2)}_{22}}{A'_{22}} \tag{A4.2b}$$

$$a'_{22} = D'^{(2)}_{22} + \frac{h'^{(2)^2}A'^{(2)}_{22}A'^{(1)}_{22}}{2A'_{22}} \tag{A4.2c}$$

$$\lambda'^2_1, \lambda'^2_2 = \frac{a'_{11}A'^{(2)}_{44}+a'_{22}A'^{(1)}_{44} \pm \sqrt{(a'_{11}A'^{(2)}_{44}+a'_{22}A'^{(1)}_{44})^2 - 4A'^{(1)}_{44}A'^{(2)}_{44}(a'_{11}a'_{22}-a'^2_{12})}}{2(a'_{11}a'_{22}-a'^2_{12})} \tag{A4.3}$$

$$p'_j = -\frac{a'_{12}\lambda'^2_j}{a'_{11}\lambda'^2_j - A'^{(1)}_{44}} \tag{A4.4}$$

$$\gamma'^{(1)}_j = \frac{p'_j(h'^{(1)}A'^{(2)}_{22}-2B'^{(1)}_{22})+h'^{(2)}A'^{(2)}_{22}}{A'_{22}} \tag{A4.5a}$$

$$\gamma'^{(2)}_j = -\frac{p'_j(h'^{(1)}A'^{(1)}_{22}+2B'^{(1)}_{22})+h'^{(2)}A'^{(1)}_{22}}{A'_{22}} \tag{A4.5b}$$

$$\eta'_j = (B'^{(1)}_{22}p'_j + A'^{(1)}_{22}\gamma'^{(1)}_j)\lambda'_j \tag{A4.6}$$

$$\xi'^{(1)}_j = (D'^{(1)}_{22} p'_j + B'^{(1)}_{22} \gamma'^{(1)}_j)\lambda'_j \quad \xi'^{(2)}_j = D'^{(2)}_{22} \lambda'_j \tag{A4.7a,b}$$

for $j = 1, 2$.

$$\theta'_1 = \frac{A'^{(1)}_{22}}{D'^{(1)}_{22} A'^{(1)}_{22} - B'^{(1)^2}_{22}} [\alpha'_1 \xi'^{(1)}_1 \cosh(s-l)) + \alpha'_2 \xi'^{(1)}_2 \cosh(\lambda'_2 (s-l))] - \frac{B'^{(1)}_{22} A'^{(2)}_{22}}{A'_{22}(D'^{(1)}_{22} A'^{(1)}_{22} - B'^{(1)^2}_{22})} N \tag{A4.8a}$$

$$\theta'_2 = -s\theta'_1 N \tag{A4.8b}$$

$$\theta'_3 = \frac{\frac{1}{2} D'^{(1)}_{22} A'_{22} - B'^{(1)^2}_{22}}{A'_{22}(D'^{(1)}_{22} A'^{(1)}_{22} - B'^{(1)^2}_{22})} - \frac{B'^{(1)}_{22}}{D'^{(1)}_{22} A'^{(1)}_{22} - B'^{(1)^2}_{22}} [\alpha'_1 \xi'^{(1)}_1 \cosh(\lambda'_1 (s-l)) + \alpha'_2 \xi'^{(1)}_2 \cosh(\lambda'_2 (s-l))] \tag{A4.8c}$$

$$\theta'_4 = \alpha'_1 \gamma'^{(1)}_1 \sinh(\lambda'_1 (s-l)) + \alpha'_2 \gamma'^{(1)}_2 \sinh(\lambda'_2 (s-l)) + \left(\frac{N}{A'_{22}} - \theta'_3\right)(s-l) \tag{A4.8d}$$

$$\psi'_1 = \frac{1}{2\omega'_1} e^{-\omega'_1 (s-l)} \sum_{j=1}^{2} \alpha'_j [\omega'_1 \sinh(\lambda'_j (s-l)) + \lambda'_j \cosh(\lambda'_j (s-l))] \tag{A4.9a}$$

$$\psi'_2 = \frac{1}{2\omega'_1} e^{\omega'_1 (s-l)} \sum_{j=1}^{2} \alpha'_j [\omega'_1 \sinh(\lambda'_j (s-l)) - \lambda'_j \cosh(\lambda'_j (s-l))] \tag{A4.9b}$$

$$\psi'_3 = 0 \tag{A4.9c}$$

References

Armanios, E. A., Sriram, P. and Badir, A. M. (1991) Fracture analysis of transverse crack-tip and free-edge delamination in laminated composites. *Composite Materials*: *Fatigue and Fracture*, *ASTM STP* **1110,** 269–286.

Crossman, F. W. and Wang, A. S. D. (1982) The dependence of transverse cracking and delamination on ply thickness in graphite/epoxy laminates. *Damage in Composite Materials*, *ASTM STP* **775,** 118–139.

Dharani, L. R. and Tang, H. (1990) Micromechanics characterization of sublaminate damage. *International Journal of Fracture* **46,** 123–140.

Fan, J. and Zhang, J. (1993) *In situ* damage evolution and micro/macro transition for laminated composites. *Composites Science and Technology* **47,** 107–118.

Fukanaga, H., Chou, T. W., Peters, P. W. M. and Schulte, K. (1984) Probabilistic failure strength analysis of graphite/epoxy cross-ply laminates. *Journal of Composite Materials* **18,** 339–356.

Han, Y. M. and Hahn, H. T. (1989) Ply cracking and property degradations of symmetric balanced laminates under general in-plane loading. *Composites Science and Technology* **31,** 165–177.

Hashin, Z. (1987) Analysis of orthogonally cracked laminates under tension. *Journal of Applied Mechanics* **54,** 872–879.

Jamison, R. D., Schulte, K., Reifsnider, K. L. and Stinchcomb, W. W. (1984) Characterization and analysis of damage mechanisms in tension–tension fatigue of graphite/epoxy laminates. *Effects of Defects in Composite Materials ASTM STP* **836,** 21–55.

Laws, N. and Dvorak, G. J. (1988) Progressive transverse cracking in composite laminates. *Journal of Composite Materials* **22,** 900–915.

Martin, R. H. and Murri, G. B. (1990) Characterization of mode I and mode II delamination growth and thresholds in graphite/PEEK composite. *Composite Materials*: *Testing and Design*, *ASTM STP* **1059,** 251–270.

Nairn, J. A. and Hu, S. (1992) The initiation and growth of delaminations induced by matrix microcracks in laminated composites. *International Journal of Fracture* **57,** 1–24.

Nuismer, R. J. and Tan, S. C. (1988) Constitutive relations of a cracked composite lamina. *Journal of Composite Materials* **22,** 306–321.

O'Brien, T. K. (1982) Characterization of delamination onset and growth in a composite laminate. *Damage in Composite Materials*, *ASTM STP* **775,** 140–167.

O'Brien, T. K. (1985) Analysis of local delaminations and their influence on composite laminate behavior. *Delamination and Debonding of Materials*, *ASTM STP* **876,** 282–297.

O'Brien, T. K. (1991) Residual thermal and moisture influences on the strain energy release rate analysis of local delaminations from matrix cracks. NASA TM-104077, AVSCOM TR-91-B-012.

Parvizi, A. and Bailey, J. E. (1978) On multiple transverse cracking in glass fiber epoxy cross-ply laminates. *J. Mater. Sci.*, **13,** 2131–2136.

Praveen, G. N. and Reddy, J. N. (1994) Stiffness reduction in composite laminates due to transverse matrix cracks. *IUTAM Symp. on Microstructure-Property Interaction in Composite Materials*, ed. R. Pyrz, pp. 301–312.

Salpekar, S. A. and O'Brien, T. K. (1991) Combined effect of matrix cracking and free edge on delamination. *Composite Materials*: *Fatigue and Fracture*, *ASTM STP* **1110,** 287–311.

Varna, J. and Berglund, L. (1991) Multiple transverse cracking and stiffness reduction in cross-ply laminates. *Journal of Composite Technology and Research*, *ICTRER* **13,** 99–106.

Xu, L.-Y. (1995) Influence of stacking sequence on the transverse matrix cracking in continuous fiber crossply laminates. *Journal of Composite Materials* **29,** 1337–1358.

Zhang, J., Fan, J. and Soutis, C. (1992a) Analysis of multiple matrix cracking in $[\pm\theta_m/90_n]_s$ composite laminates: Part I, in-plane stiffness properties. *Composites* **23,** 291–298.

Zhang, J., Fan, J. and Soutis, C. (1992b) Analysis of multiple matrix cracking in $[\theta\pm_m/90_n]_s$ composite laminates: Part II, development of transverse ply cracks. *Composites* **23,** 299–304.

Zhang, J., Soutis, C. and Fan, J. (1994) Strain energy release rate associated with local delamination in cracked composite laminates. *Composites* **25,** 851–862.